Final Report
Non-Linear Seismic Site Response of Deep Deposits in West Tennessee

Prepared for
Tennessee Department of Transportation

Principal Investigators:

Youssef Hashash
Assistant Professor
University of Illinois at Urbana-Champaign

Shahram Pezeshk,
Professor
The University of Memphis

Graduate Research Assistant:
Duhee Park
Graduate student
University of Illinois at Urbana-Champaign

Tuesday, January 27, 2004

DRAFT

Table of Contents

List of Tables

List of Figures

1. Introduction

1.1. Background

The deep soil deposits of the Mississippi embayment have a pronounced yet not fully understood influence on the amplification and attenuation of ground motions associated with the New Madrid seismic zone (NMSZ). The NMSZ is considered capable of producing large earthquakes (M>7.0). In the embayment there is an absence of recorded ground motions of significant level (M>5.0). The embayment is a trough like depression that plunges southward along an axis that approximates the course of the Mississippi River, Figure 1-1. As shown in Figure 1-2, the embayment is filled with sediments of clay, silt, sand, and gravel to depths reaching 500 meters to 1000 meters.

In a study by Pezeshk et al. (1998) titled "Seismic Acceleration Coefficients for West Tennessee" a detailed analysis of the seismic hazard potential and the influence of local soils on anticipated ground motion levels are presented. Since this study several advances have been made in the assessment of seismic hazard including:

1. Development of a new one-dimensional non-linear wave propagation model (*DEEPSOIL*) to evaluate the amplification/attenuation characteristics of the deep soil deposits. The newly developed model is specifically designed to account for the effect of confining pressure on shear modulus and damping characteristics of soil deposits. The new model shows that the propagated motions are significantly higher than would be obtained using conventional models (Hashash and Park, 2001, Hashash and Park, 2002, Park and Hashash, 2003). Preliminary analyses using this model show that there is significant amplification of long period waves through the thick deposits of the embayment. The deep deposits are capable of transmitting some high frequency components of the ground motion as well.
2. Development of additional information regarding the geology of the Mississippi embayment.
3. Development of additional information on seismicity in the New Madrid seismic zone.

1.2. Probabilistic seismic hazard analysis (PSHA)

The seismic hazard from a PSHA is an aggregate risk from potential earthquakes of many different magnitudes occurring at many different source-site distances. Each of the potential earthquake scenarios is different in terms of its ground motion parameters, such as PGA and spectral accelerations. The site coefficients, defined as a function of the ground motion parameters, will be different for the various earthquake scenarios. Applying different site coefficients for different ground motions will preserve the probabilistic nature of the PSHA. This is seldom done in practice and the combined sum of the future seismic hazards, represented in selected ground motion parameters, is treated as originating from a single source (e.g. NEHRP).

1.3. Proposed procedure to develop probabilistic site coefficients

In this study typical profiles in West Tennessee are selected to determine whether the new developments will result in different acceleration coefficients compared to the National Earthquake Hazard Reduction Program (NEHRP). The accuracy and the conservatism of the NEHRP amplification factors are assessed.

The proposed procedure to develop fully probabilistic site coefficients, is illustrated in Figure 1-3 and comprises five main steps:

Step 1: Selection of site locations, site profiles, and dynamic properties (Sections 2 and 3).

Step 2: Generation of suites of ground motion time series: The motions when use in probabilistic seismic hazard analysis results in a uniform hazard spectra that match the USGS B/C hazard maps. The procedure is discussed in Section 4.

Step 3: Conversion of B/C motions to hard rock motions: The generated motions are then converted to hard rock motions for use in site response analysis.

Step 4: Site response analysis: The suite of hard rock motions is propagated through Uplands and Lowlands and site specific profiles (Section 3). The characteristic ground motions are propagated using nonlinear analysis. The ground motions from gridded seismicity are propagated using equivalent linear analysis. Both the nonlinear and equivalent linear analyses are performed using DEEPSOIL. The response spectra of the motions are used to develop the uniform hazard response spectrum.

Step 5: Determination of probabilistic site coefficients: Probabilistic site coefficients are computed as the ratio of the surface uniform hazard response spectrum (UHRS) to the B/C boundary UHRS (Section 5).

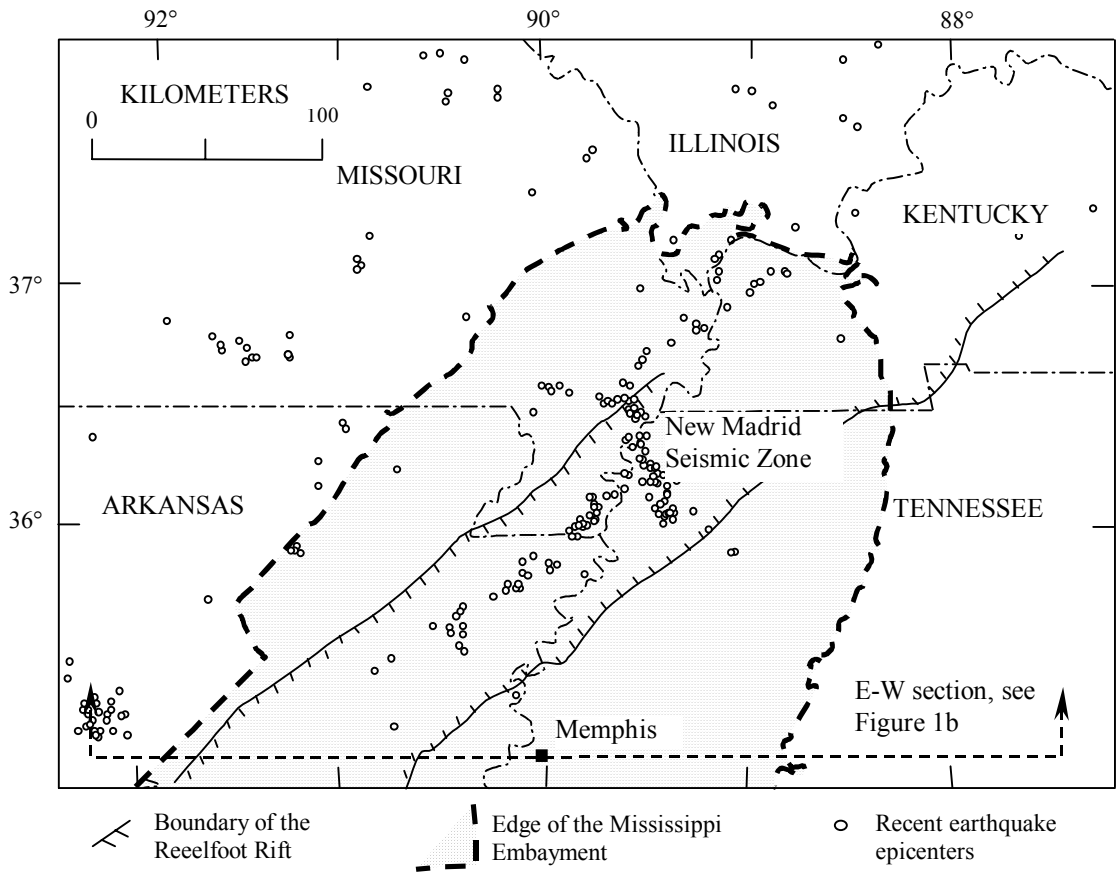

Figure 1-1. Plan view of the Mississippi embayment (after Ng et al., 1989).

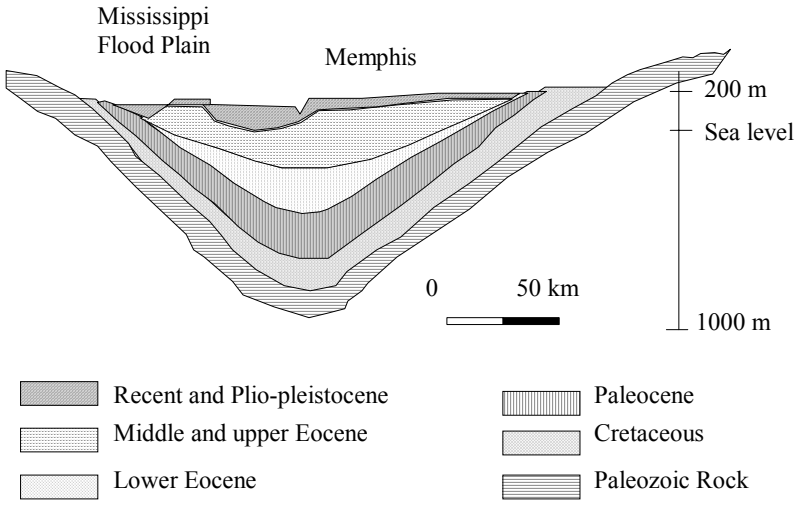

Figure 1-2. East-west profile view of the Mississippi embayment through Memphis and Shelby County (after Ng et al., 1989).

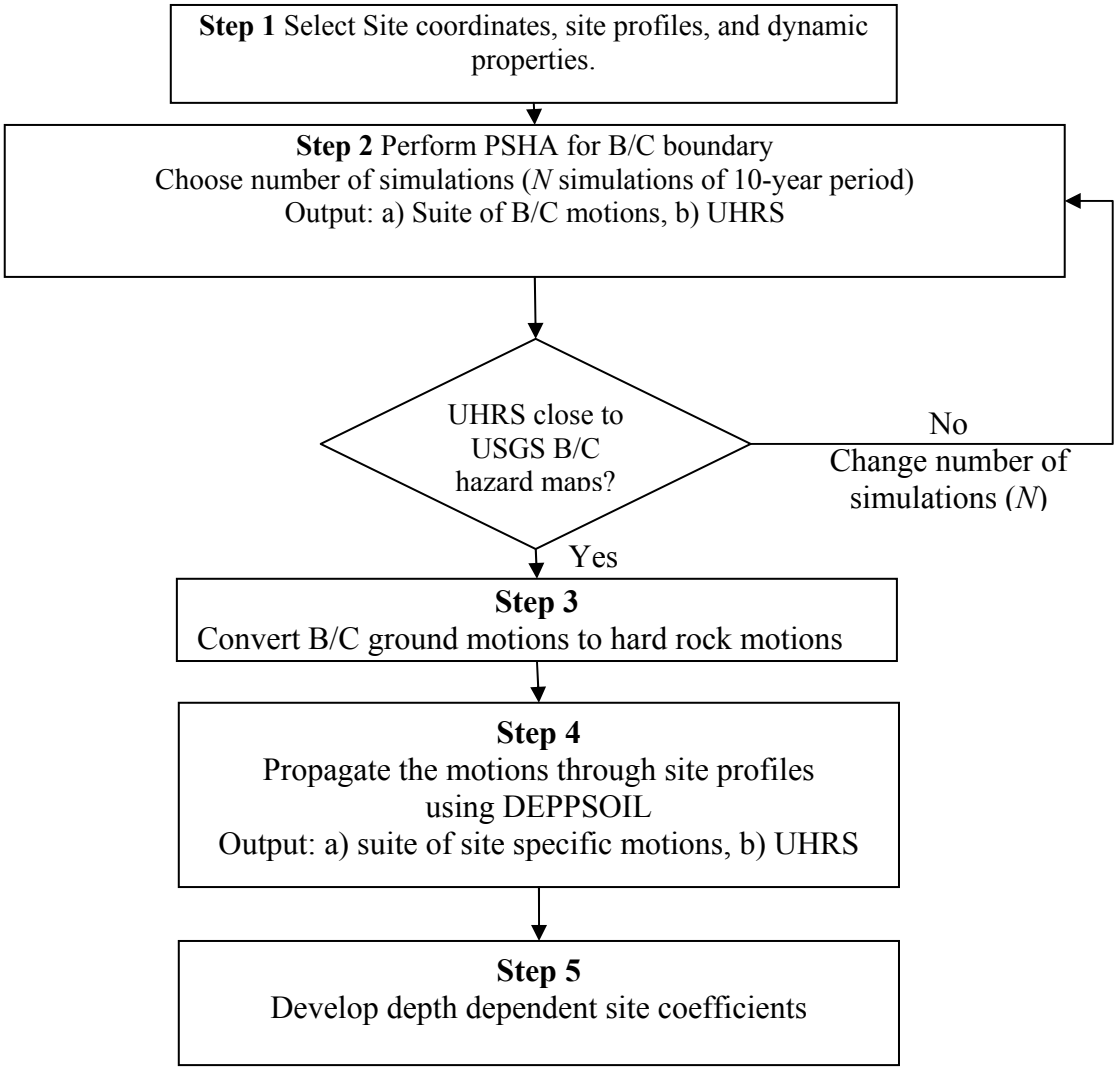

Figure 1-3. Probabilistic site coefficients estimation procedure flowchart.

2. Selection of Study Sites

Several sites in West Tennessee are considered in this study. Table 2-1 and Figure 2-1 provide the locations of all sites considered in this study as well as the depth of unconsolidated soil deposits using a database developed by Van Arsdale and TenBrink (2000). All these sites are located within the Mississippi embayment.

2.1. NEHRP/NCHRP Site Classification and Factors

According to the NCHRP Specs Section 3.4.1 (similar to NEHRP provisions FEMA, 1997),), design response spectra (Figure 2-2) for the MCE and the expected earthquake shall be constructed using the accelerations from national ground motion maps. Design earthquake response spectral accelerations at short periods, S_{DS}, and at 1-second period, S_{D1}, are determined by:

$$S_{DS} = F_a S_s \tag{2-1}$$

and

$$S_{D1} = F_V S_1 \tag{2-2}$$

where S_s and S_1 are the 0.2-second period spectral acceleration and 1-second period spectral acceleration, respectively, on Class B rock (Table 2-2) from ground motion maps and F_a and F_v are site coefficients as given in Table 2-3 and Table 2-4, respectively.

According to NCHRP Specs Table 3.4.2-1 (Table 2-2 given below) titled "Site Classification," a site class B is a rock site with average shear wave velocity of top 100 ft (30 m) of soil to be 2500 ft/s < V_s< 5000 ft/s or 760 m/s < V_s< 1500 m/s. Similarly, a site class C is a very dense soil and soft rock with 1200 ft/s < V_s< 2500 ft/s or 360 m/s < V_s< 760 m/s. Therefore, a B-C boundary would be a soil profile having an average shear wave velocity of 2500 ft/sec or 760 m/s. In West Tennessee, in particular, in Memphis, the B/C boundary is located approximately 1000 ft below the ground surface (Pezeshk et al., 1998). Therefore, using site coefficients F_a and F_v, which are for only the top 100 ft of soil, is not appropriate in West Tennessee.

2.2. Classification of Sites Studied

The boring logs of the sites studied are used to determine site class for each location. Boring logs of all the sites studied can be found in Pezeshk et al. (1998). Table 2-5 provides a summary of SPT *N* values for all the sites studies. The soil classification for each site is determined at the bottom of Table 2-5.

Table 2-1. Sites Considered in this Study.

Site Name	Latitude	Longitude	Depth (m)
Route 14	89.824	35.308	750
Somerville	89.359	35.279	530
Covington	89.625	35.400	710
Brownsville	89.260	35.539	525
Newbern	89.248	35.138	440
Jackson	88.920	35.635	350
Trenton	88.947	35.965	460
Paris	88.336	36.267	50
Wynnburg	89.475	36.321	600

Table 2-2. Site Classification.

Soil Profile Type	**Description**	$\overline{V_s}$ **(ft/sec)**	$\overline{S_u}$ **(psf)**
A	Hard Rock	$\overline{V_s} > 5000$	
B	Rock		
C	Very Dense Soft Rock $\overline{N} > 50$	$2500 < \overline{V_s} \leq 5000$	$\overline{S_u} \geq 2000$
D	Stiff Soil $15 < \overline{N} < 50$	$1200 < \overline{V_s} \leq 2500$	$1000 < \overline{S_u} \leq 2000$
E	PI>20 W> 40	$600 < \overline{V_s} \leq 1200$	$\overline{S_u} \leq 500$
F	Need Site Specific Study		

S_u=undrained Shear Strength
PI = Plastic Index
N = Standard penetration Resistance

Table 2-3. Values of F_a as a Function of Site Class and Mapped Short-Period Spectral Acceleration.

Site	Mapped Maximum Considered Earthquake Spectral Response Acceleration at Short Period				
	$S_S <$	S_S	S_S	S_S	S_S
A	0.8	0.8	0.8	0.8	0.8
B	1.0	1.0	1.0	1.0	1.0
C	1.2	1.2	1.1	1.0	1.0
D	1.6	1.4	1.2	1.1	1.0
E	2.5	1.7	1.2	0.9	a
F	A	a	a	a	a

Table 2-4. Values of F_v as a Function of Site Class and Mapped 1 Second Period Spectral Acceleration.

Site	Mapped Maximum Considered Earthquake Spectral Response Acceleration at 1 Second Period				
	$S_1 <$	S_1	S_1	S_1	S_1
A	0.8	0.8	0.8	0.8	0.8
B	1.0	1.0	1.0	1.0	1.0
C	1.7	1.6	1.5	1.4	1.3
D	2.4	2.0	1.8	1.6	1.5
E	3.5	3.2	2.8	2.4	A
F	a	a	a	a	a

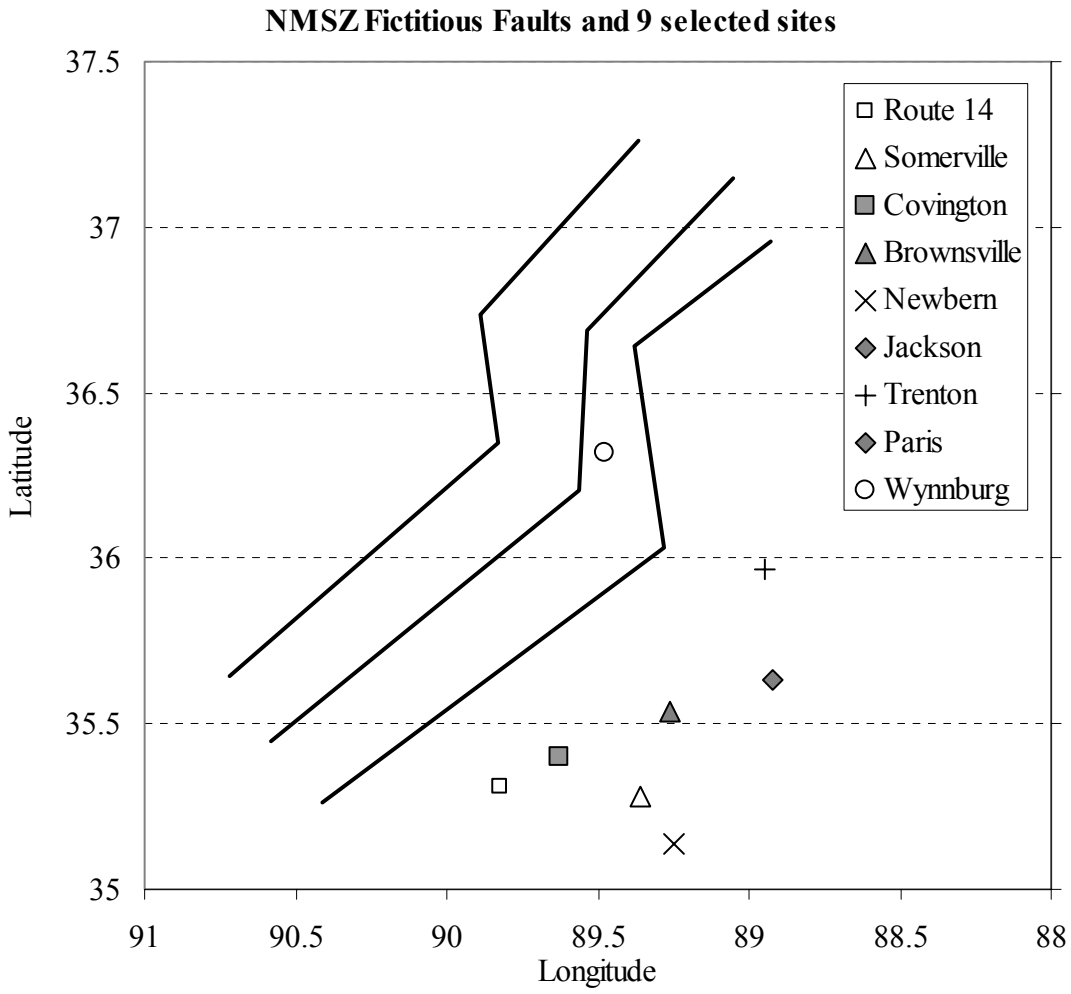

Figure 2-1. Sites considered in this study.

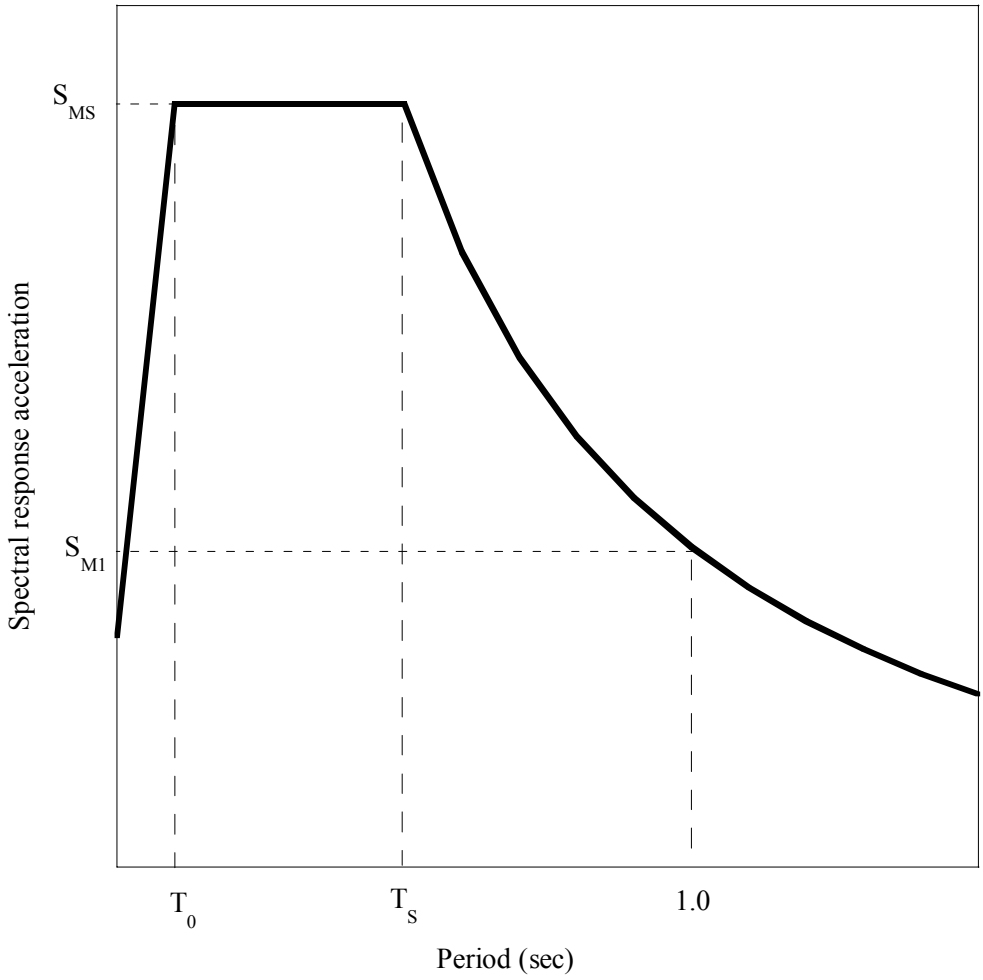

Figure 2-2. NEHRP recommended response spectrum.

Table 2-5. Blow Counts at Various Depths for the Study Sites.

Depth	Thickness	Route 14	Somerville	Covington	Brownsville	Newbern	Jackson	Trenton	Paris	Wynnburg
5	5	8	34	8	17	10	18	9	14	11
10	5	10	34	8	19	4	24	10	30	7
15	5	10	39	6	17	6	22	10	31	4
20	5	14	38	9	17	6	40	13	37	3
25	5	11	40	9	32	65	9	13	36	39
30	5	12	41	21	26	90	12	24	67	36
35	5	13	43	20	21	111	34	24	79	43
40	5	33	40	30	21	125	46	26	100	48
45	5	39	33	30	17	357	51	22	62	19
50	5	97	67	69	33	321	14	19	100	18
55	5	60	89	74	35	239	57	77	100	32
60	5	55	78	79	55	72	63	87	76	41
65	5	62	75	79	45	62	29	39	100	23
70	5	17	97	69	35	59	152	10	100	28
75	5	22	89	59	181	107	200	20	32	33
80	5	19	87	55	164	104	184	26	42	39
90	10	52	95	55	215	103	200	82	15	48
100	10	82	97	53	92	107	200	64		58
Average N Value		**20**	**55**	**20**	**32**	**24**	**33**	**20**	**37**	**16**
Site Class		**D**	**C**	**D**	**D**	**D**	**D**	**D**	**D**	**D**

3. DEEPSOIL and Dynamic Properties for Site Response Analysis

An important feature of this study is the use of a new site response analysis code DEEPSOIL to simulate the influence of the very deep unconsolidated embayment deposits on the the propagated ground motion. This section provides a brief description of DEEPSOIL and the dynamic soil properties selected for the 9 sites in western Tennessee. These properties are used in developing the input for DEEPSOIL

3.1. DEEPSOIL: Site response analysis program

DEEPSOIL is a new one-dimensional (1-D) site response analysis program developed to accurately simulate wave propagation through very deep deposits. A detailed description of the model can be found in (Hashash and Park, 2001; Hashash and Park, 2002; Park and Hashash, 2003). The model incorporates several important enhancements over conventional site response analysis programs:

1. Non-linear time domain analysis:
    a. Pressure dependent modified hyperbolic soil model: In non-linear analysis a new confining pressure dependent nonlinear hyperbolic soil model is used. The model accounts for the change in dynamic soil properties due to increasing soil depth.
    b. Viscous damping formulation: In non-linear analysis, viscous damping is often used to represent soil damping at zero strain as most soil constitutive models are nearly linear at very small strain strains. The program includes a new viscous damping formulation to reduce the artificial damping introduced numerically through uncontrolled frequency dependent viscous damping.
    c. Numerical integration: The program includes a new numerical integration scheme to increase numerical accuracy and efficiency in modeling the nonlinear behavior of the soil.
2. Equivalent linear frequency domain analysis: When performing equivalent linear frequency domain analysis the user can use an unlimited number of layers and material types. This removes the limitations found in several existing programs such as SHAKE'91.

The use of the non-linear analysis is appropriate for propagation of strong ground motion while the equivalent linear analysis is appropriate for propagation of weaker motion. In order to perform a non-linear or an equivalent linear site response analysis material properties have to be selected for the site(s) of interest.

3.2. Shear wave velocity profile

Romero et al. (2001) classified the embayment into two categories (Figure 3-1) based on geologic age. Holocene-age deposits (termed Lowlands) are found along the floodplains of the Mississippi River and its tributaries whereas Pleistocene-age deposits (termed Uplands) are located in the interfluve, terrace regions. Generic shear wave velocity profiles are developed for these two categories (Figure 3-2). The Lowlands profile shows lower shear velocity at the upper 70 m compared to the Uplands profile. The profiles are identical below 70 m. The site response

analyses performed in this study use the generic profiles as well interpreted site-specific shear-wave velocity profiles obtained from Pezeshk et al. (1998).

3.3. Zero-strain viscous damping profile

During the Enola Earthquake (M = 4.5, 1999), recordings were made in the Mississippi embayment at 9 stations ranging in thickness from 250 m to 720 m. The earthquake generate very weak motion, the soil response was primarily linear. In the absence of other embayment specific data, the recordings were used to back-calculate the viscous damping properties. The viscous damping profile has a damping ratio of 3.5 % at the surface and 0.4 % at the bottom of the 1000 m profile (Figure 3-3). The proposed viscous damping profile is higher than the profile developed by EPRI (1993).

3.4. Dynamic soil property characterization

The laboratory tests performed by Laird and Stokoe (1993) and Chang et al. (1989), have been used to develop the confining pressure dependent soil model and to characterize the confining pressure dependent soil curves.

While the laboratory tests results by Chang et al. (1992) are a valuable resource for characterizing the soil of Mississippi embayment, it is difficult to estimate the soil behavior at greater depths/higher confining pressure due to low confining pressures under which the soil samples were examined.

Laird and Stokoe (1993) performed resonant column and torsional shear tests at strain levels up to 10^{-3} and confining pressures up to 3.5 MPa using remolded sand specimens (washed mortar sand). Low and high amplitude cyclic torsional shear and resonant column tests were used to determine the effect of strain amplitude and confinement on shear modulus and damping curves. Measurements show that increase in confining pressure results in lesser shear modulus degradation at a given cyclic shear strain. Confining pressure increase has a significant influence on damping as well. Small strain damping decreases with an increase in confining pressure due to an increase in number of particle contacts, which is the main factor that dissipates energy at low amplitude strain. Based on the tests by Laird and Stokoe, EPRI (1993) proposed design curves for cohesionless soils in the general range of gravelly sands to low plasticity silts or sandy clays.

The viscous damping properties, or damping ratios at small strains, from the laboratory test data are not used. Instead, the viscous damping properties back calculated from the weak motion recordings were utilized. The viscous damping properties are higher than the laboratory test data because there are other mechanisms responsible for wave attenuation such as wave scattering. Such complex mechanisms are indirectly accounted for by using the viscous damping.

Since the viscous damping properties can be separated from hysteretic damping, the viscous damping back-calculated can be added to the hysteretic damping estimated from laboratory tests or available generic curves. In this process, the original viscous damping values should be removed so that only the hysteretic damping is added. The resulting modulus degradation and damping curves are shown in Figure 3-4.

3.5. Comparison of the estimated dynamic soil curves with the Mississippi embayment soils

The developed curves are compared/calibrated to results of actual testing of the embayment soils, performed by Chang et al. (1989). Chang et al. (1989) collected 35 soil

samples in the northern Mississippi embayment region and the samples were tested through use of resonant column. The range of soil groups sampled includes alluvial sands, sands and gravels, silty to sandy clays, and loess. Soils have been categorized into 9 groups (Table 2-1). The resonant column tests have been performed under confining pressures of 5, 20, 55, and 60 psi to determine the effect of confining pressure. The laboratory test results have been incorporated in defining the dynamic soil curves.

Figure 3-5 to Figure 3-10 show the developed dynamic curves and the laboratory test data for 6 soil groups tested by Chang et al. (1989). Figure 3-5 to Figure 3-7 compares cohesionless soils (soil groups A1 to A3) to the proposed dynamic curves. G/G_{max} curves agree well with the developed curves for all three soil groups. The developed curves are conservative showing more confining pressure dependency than the laboratory test data. The viscous damping is near the upper bound of the embayment soils. The shapes of the hysteretic damping components of the damping curves are very similar.

The cohesive soils show less pressure dependency than cohesionless soils, as shown in Figure 3-9 to Figure 3-10. The overall G/G_{max} shapes deviate from cohesionless soils, showing more pronounced S shaped curvature. The viscous damping is much higher than cohesionless soils, and is as high as 9% for the upper bound curves.

The embayment stratigraphy shown in Figure 1-2 is complex with alternating layers of sands and clays. In addition, the depths of the layers change along the embayment, making it impossible to assign depths to alternating layers. In addition, the clay samples (B1 and B2) do not represent the deep clay layers, since the high confining pressure would highly alter the characteristics of the soils and the surface clay soils cannot be used to estimate the behavior of deep clay layers. Therefore, instead of using different soil curves for different layers of soil in the embayment, the proposed curves, developed using cohesionless soils, are used throughout the profile.

3.6. Evaluation of Nonlinear Analysis vs. Equivalent Linear Analysis Site Response Analysis.

To determine how the nonlinear results are different than the current state-of-practice, which is based on the equivalent linear analysis, we performed both analyses for a site in West Tennessee (Covington, Tennessee). The following is a discussion of the results.

In this example, combinations of two ground motions (Cov_1Hz_1 and Cov_5Hz_1) and two soil profiles are used (126ft and 1738 ft). Same values of shear velocity as B/C boundary (760 m/sec) is used below the soil profile.

Both the nonlinear results from DEEPSOIL and the equivalent linear are presented in Figure 3-11 through Figure 3-14. The comparison between the shallow profile (126 ft) and deep profile (1738 ft) is pronounced at certain frequencies. At deep profiles, the spectral amplification is much lower than shallow profiles. At long periods (>1 sec), relevant for long structures, the equivalent linear analysis underestimates the surface response. At short periods (<0.1 sec) the equivalent linear analysis overestimates the surface response.

Table 3-1. NMSZ soil groups used in laboratory tests by Chang et al. (1992).

Soil Group	Description	Range of Depth of Boring (ft)
A1	Alluvial sand (SP-SM)	5'- 40'
A2	Terrace sand and gravel (SP-SW-SM-SC-GP)	5'- 44'
A3	Jackson fine sand (SP)	25-71'
B1	Silty to sandy clay (CL)	1-33'
B2	Jackson clay (CL-CH)	8'-25'
C	Loess	4.5-53.6'

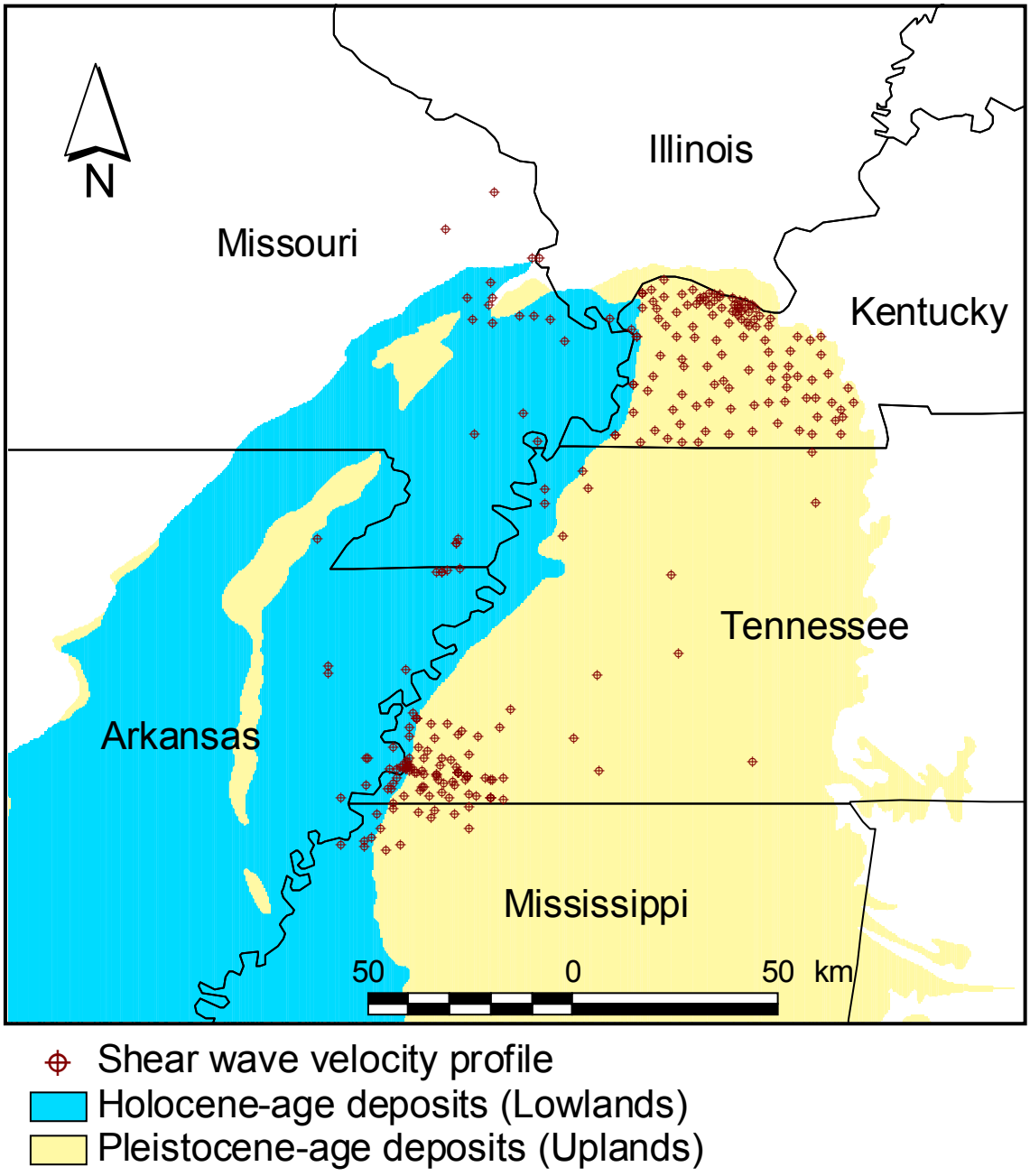

Figure 3-1. Lowlands and Uplands classification of Mississippi embayment according to Romero and Rix (2001).

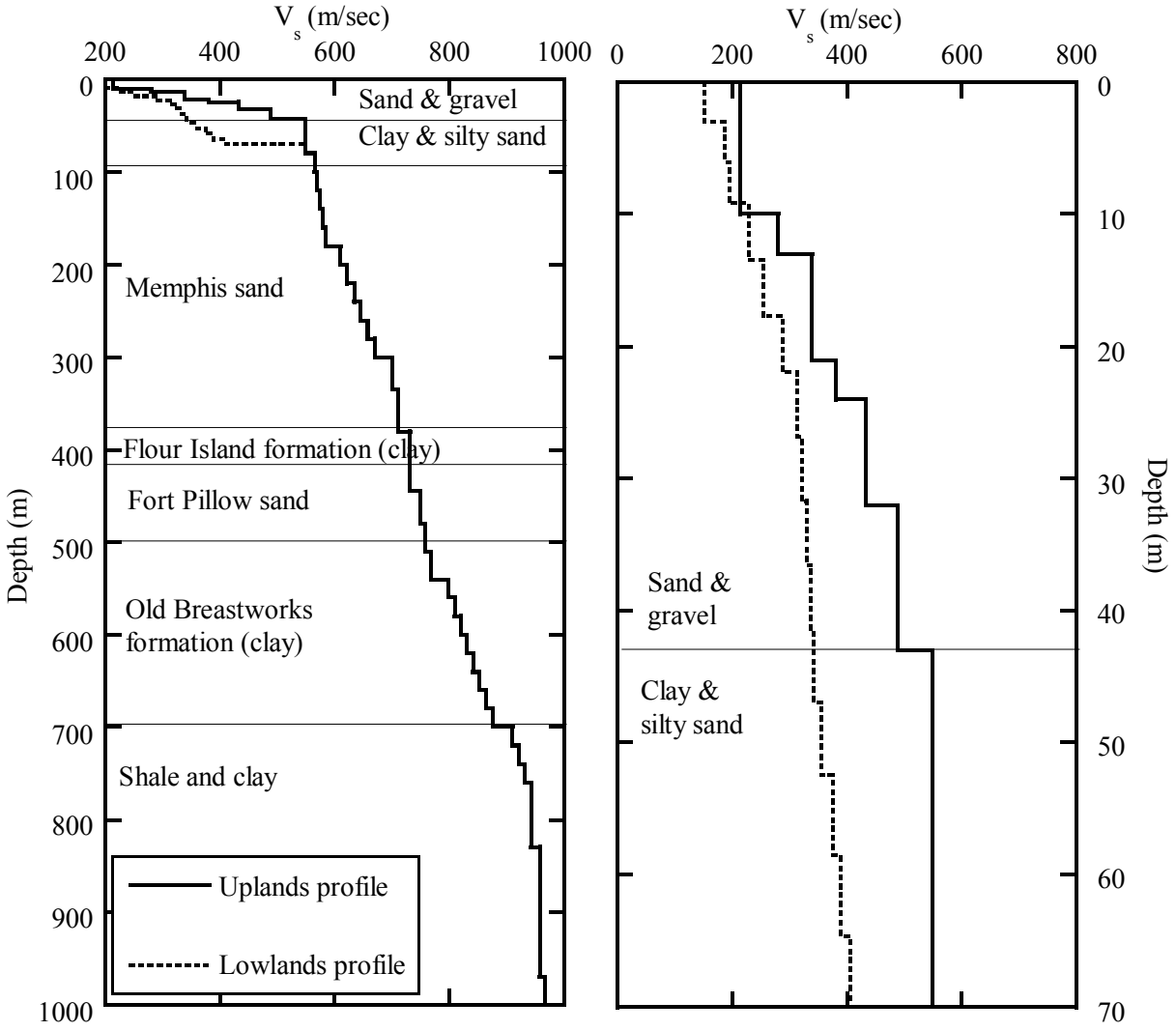

Figure 3-2. Shear wave velocity profiles of the Mississippi embayment after Romero and Rix (2001).

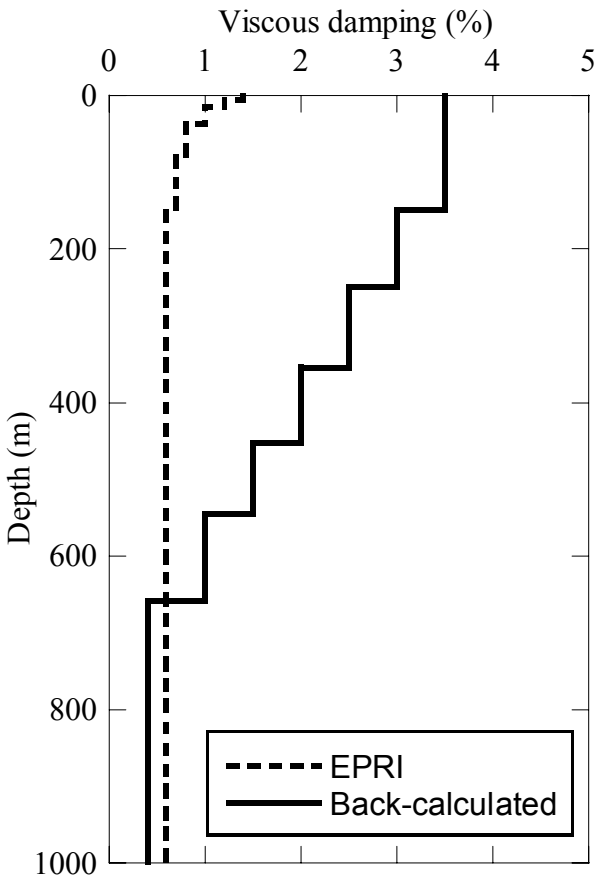

Figure 3-3. Comparison of a) back-calculated viscous damping profile and b) profile developed by EPRI (1993).

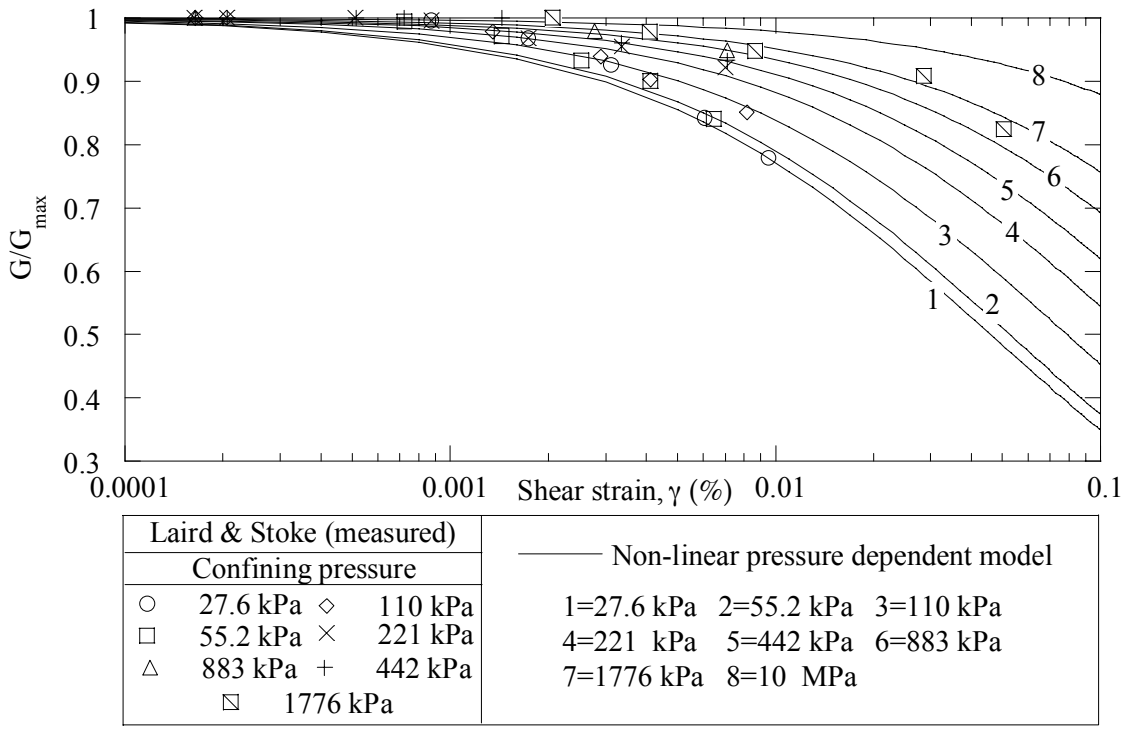

(a) Modulus degradation curves

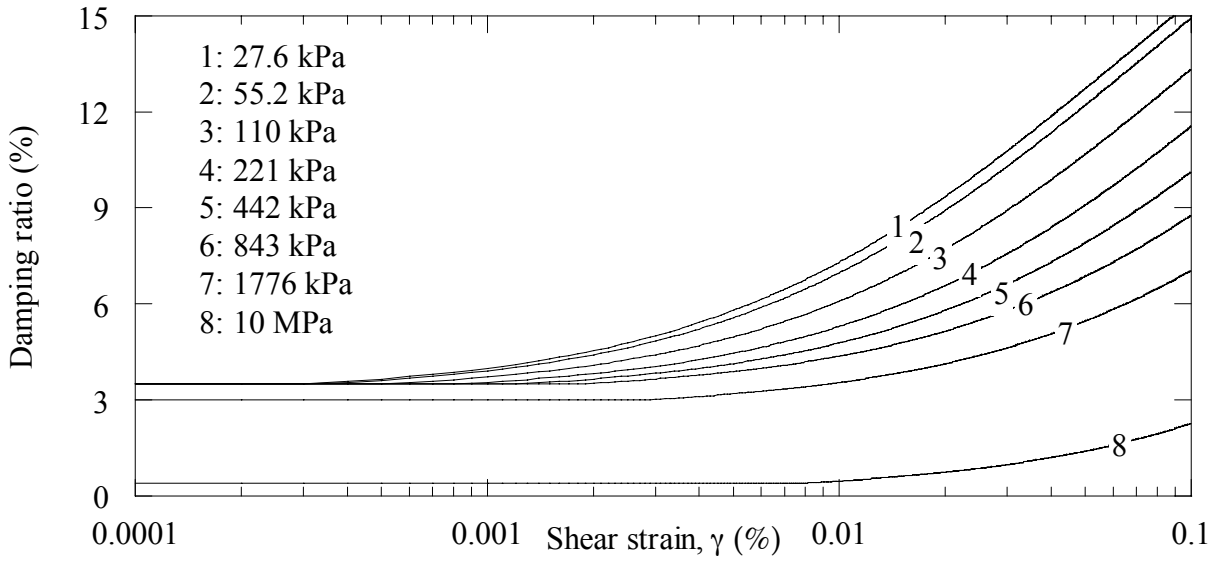

(b) Damping ratio curves from confining pressure dependent model combined with back-calculated viscous damping.

Figure 3-4. Influence of confining pressure on modulus degradation and damping ratio of soil. data points are from Laird and Stokoe (1993) and lines represent the nonlinear soil model used in DEEPSOIL (Hashash and Park 2001).

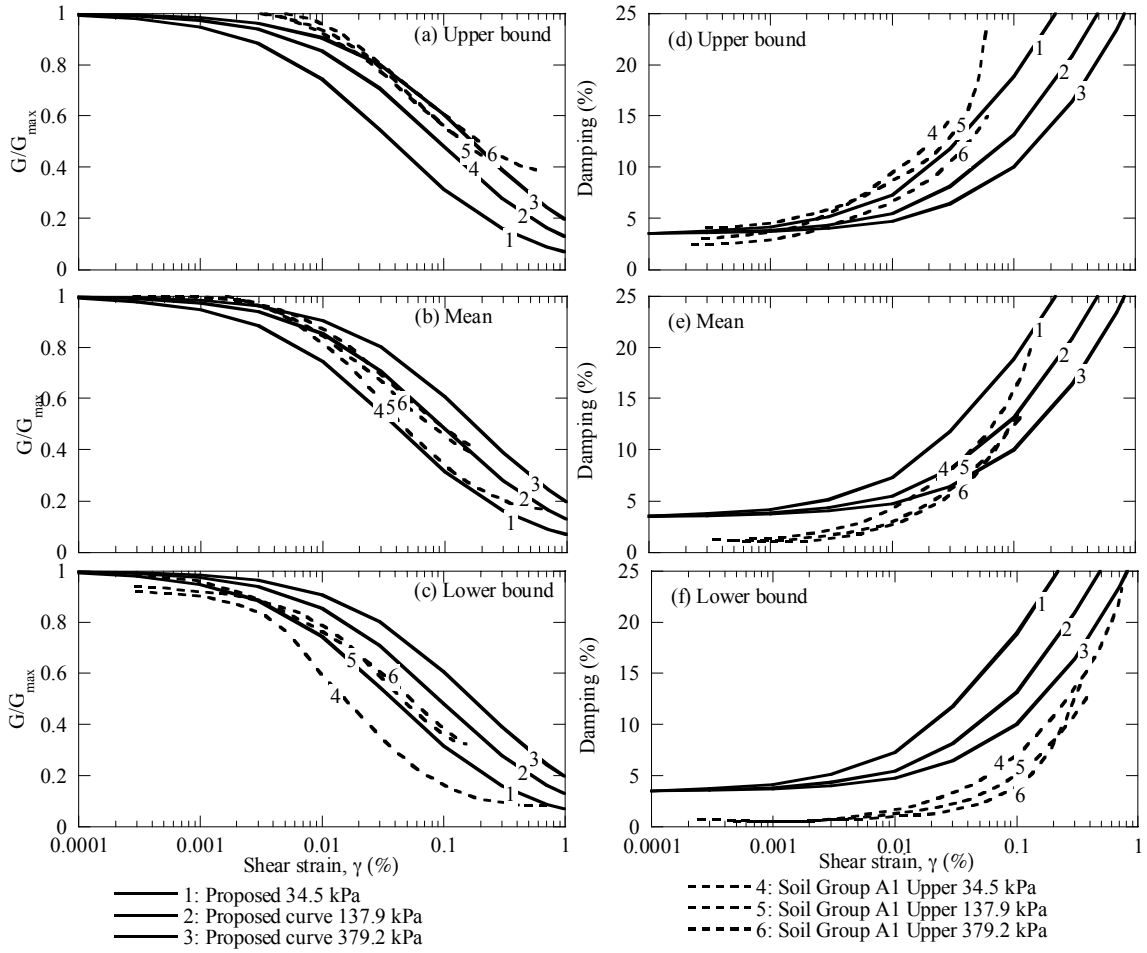

Figure 3-5. Comparison of the proposed dynamic material properties with the laboratory test data of soil group A1 by Chang et al. (1989).

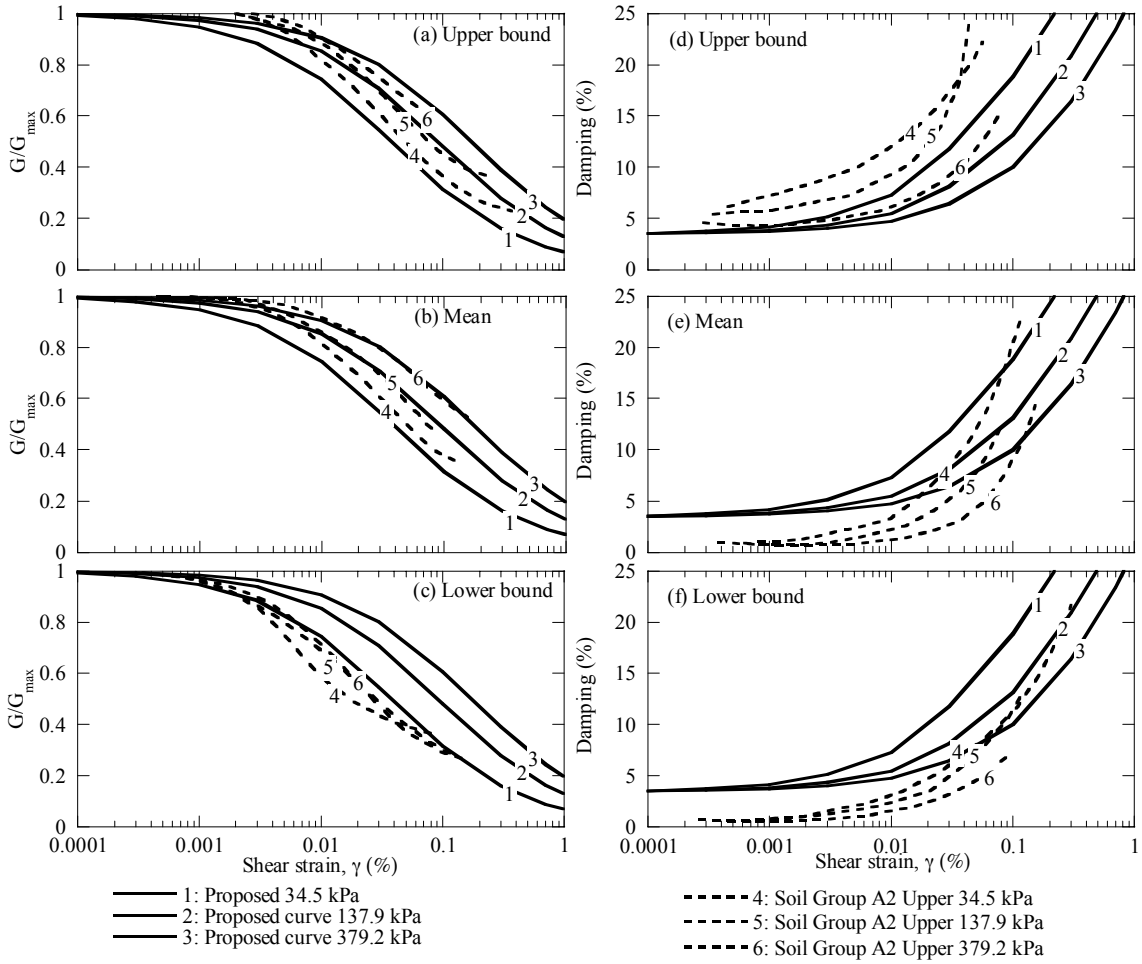

Figure 3-6. Comparison of the proposed dynamic material properties with the laboratory test data of soil group A2 by Chang et al. (1989).

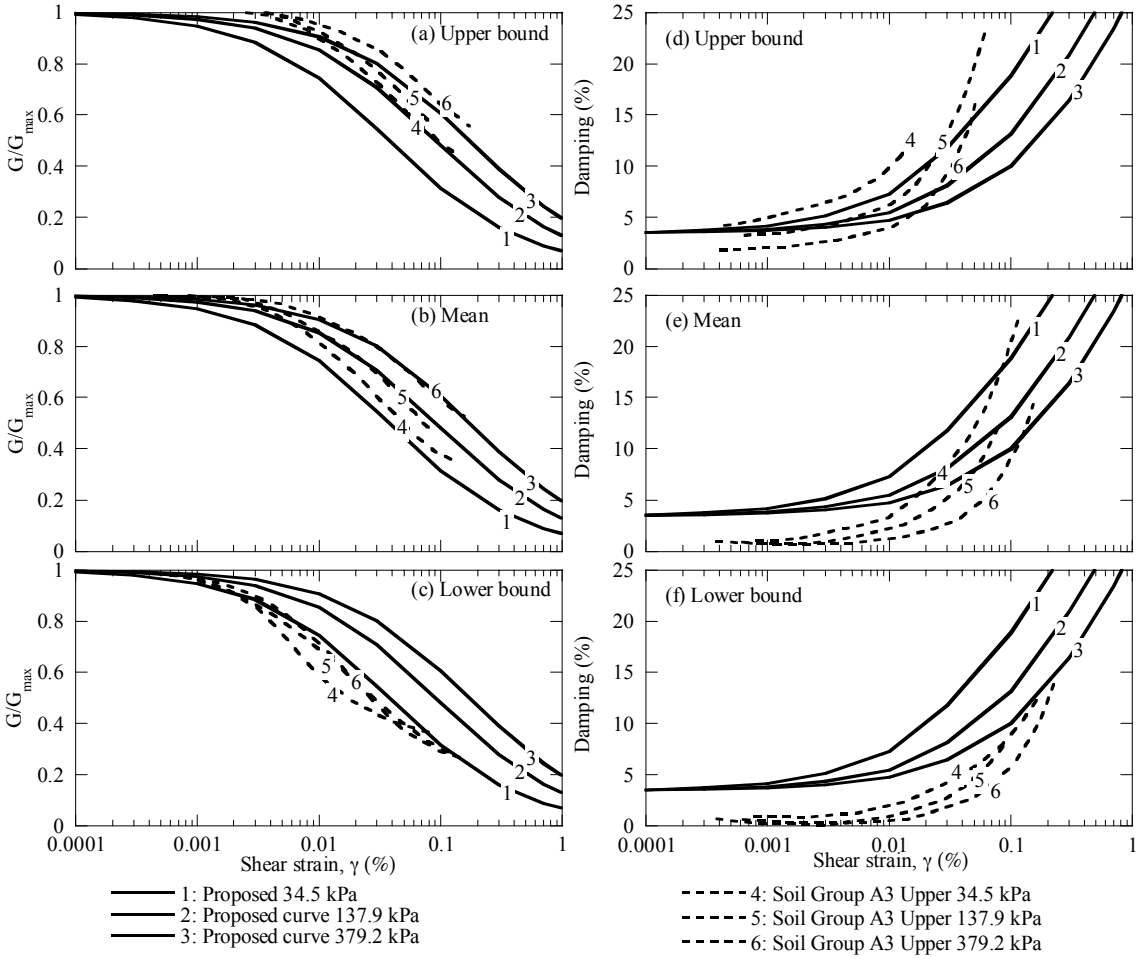

Figure 3-7. Comparison of the proposed dynamic material properties with the laboratory test data of soil group A3 by Chang et al. (1989).

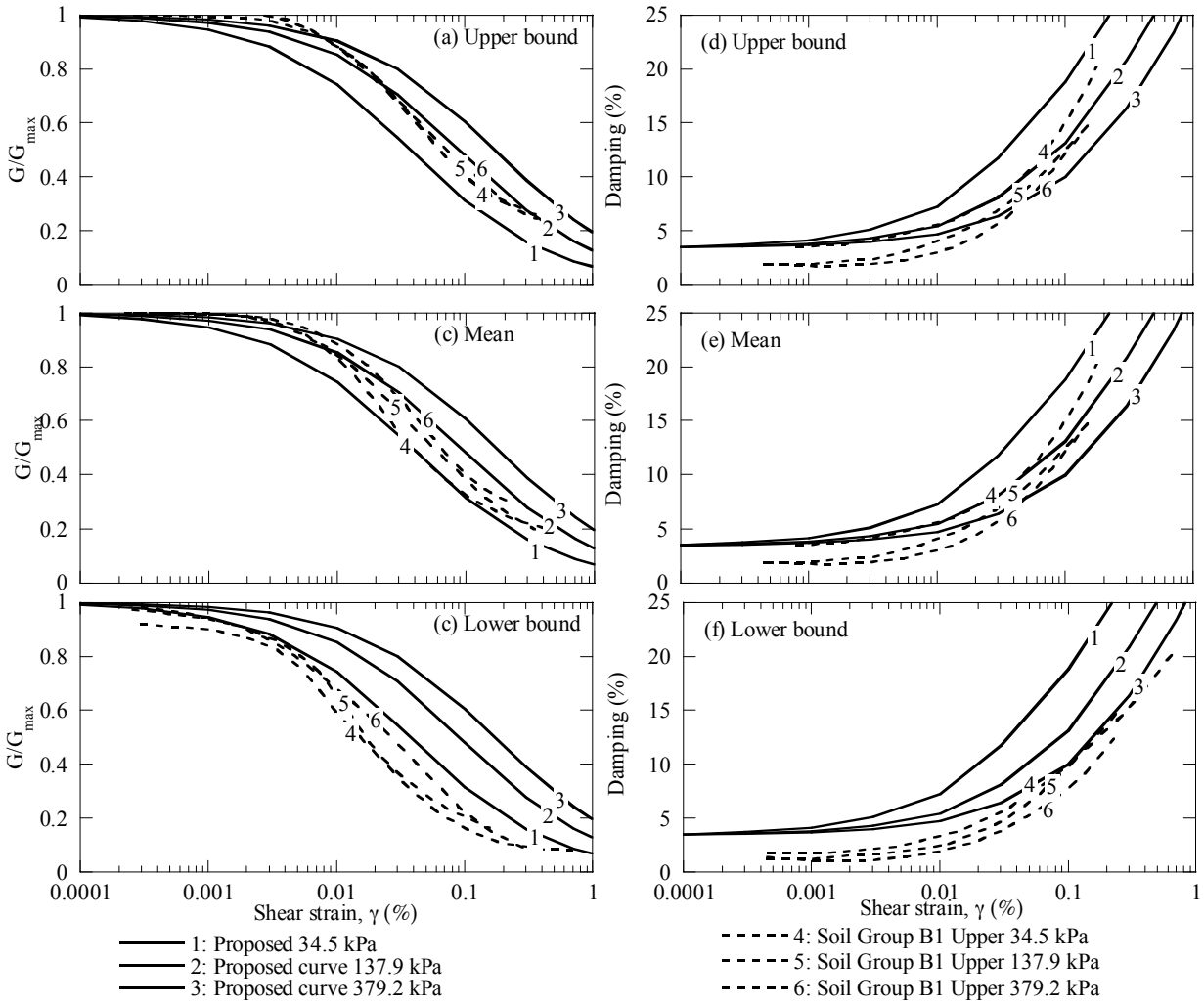

Figure 3-8. Comparison of the proposed dynamic material properties with the laboratory test data of soil group B1 by Chang et al. (1989).

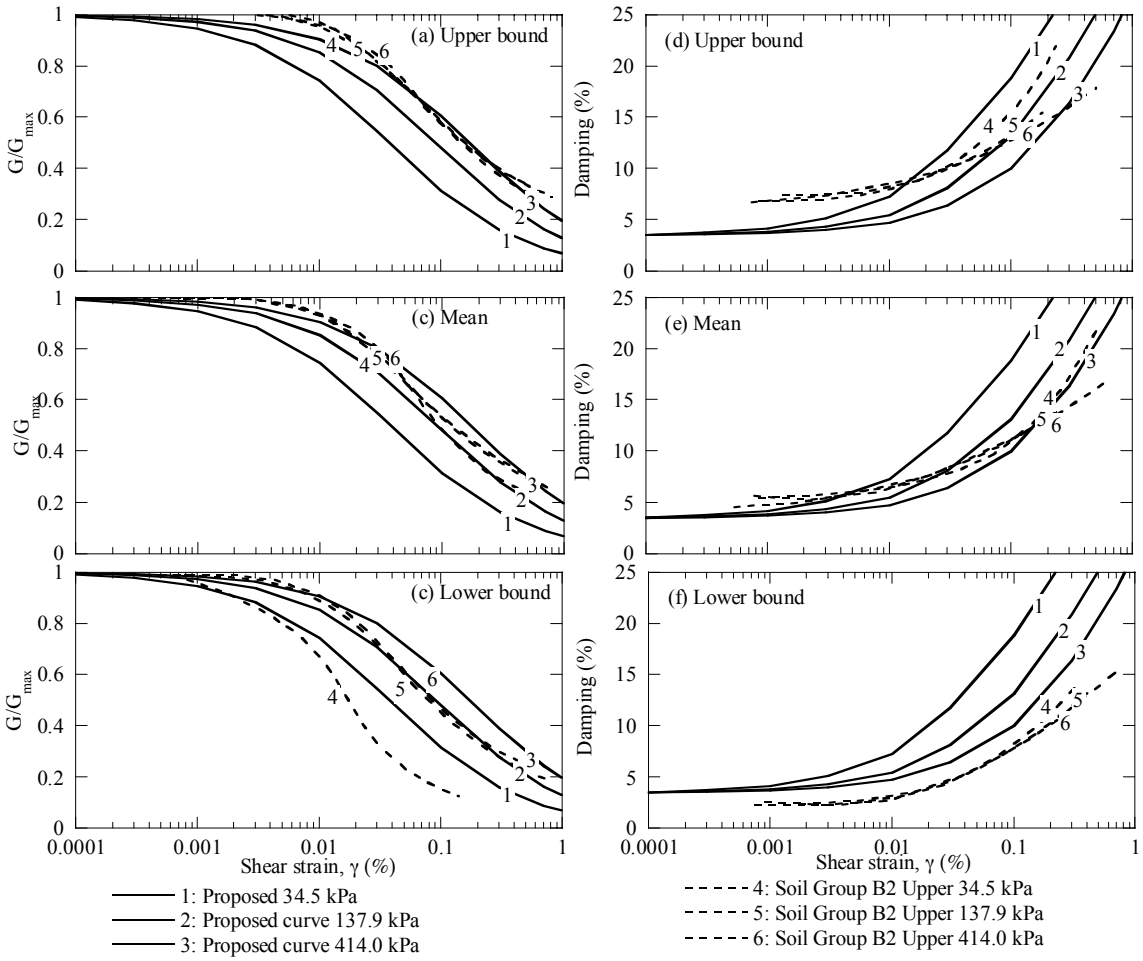

Figure 3-9. Comparison of the proposed dynamic material properties with the laboratory test data of soil group B2 by Chang et al. (1989).

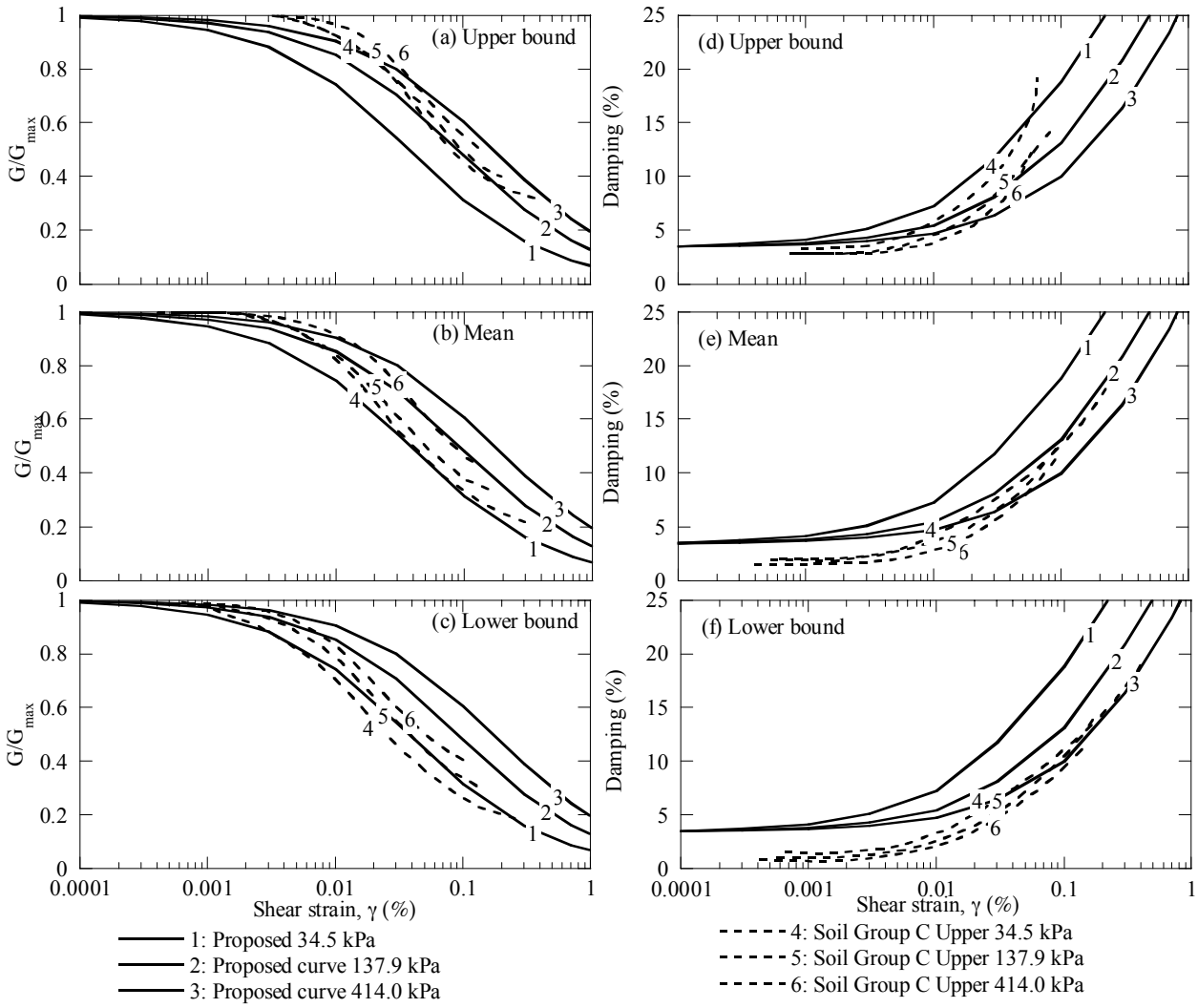

Figure 3-10. Comparison of the proposed dynamic material properties with the laboratory test data of soil group C by Chang et al. (1989).

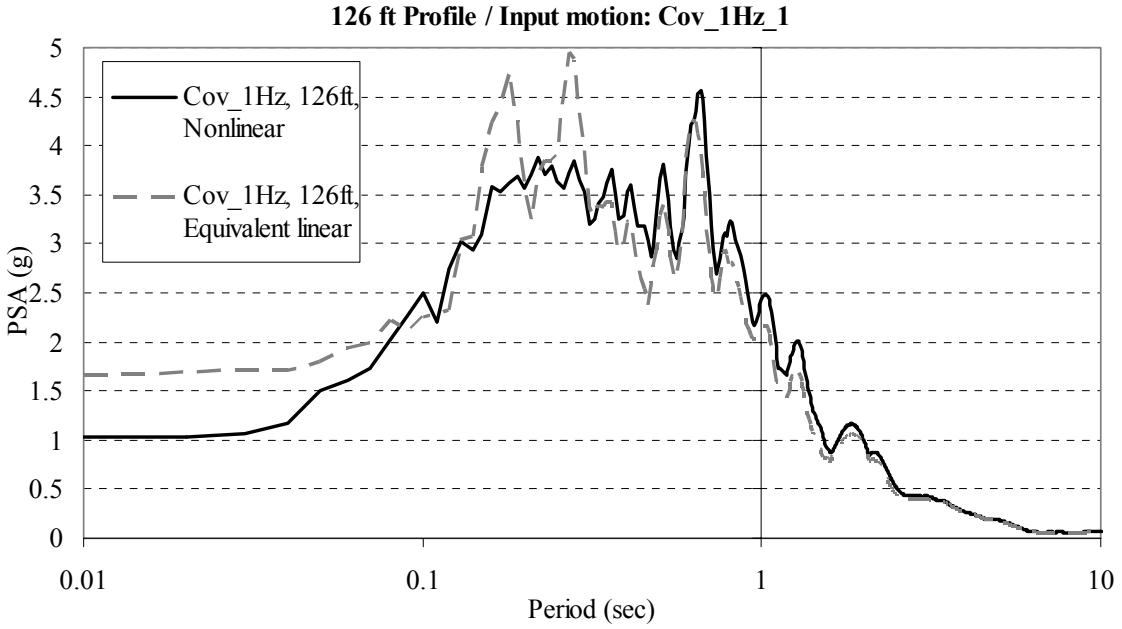

Figure 3-11. 126-ft profile using time histories generated using 1Hz case.

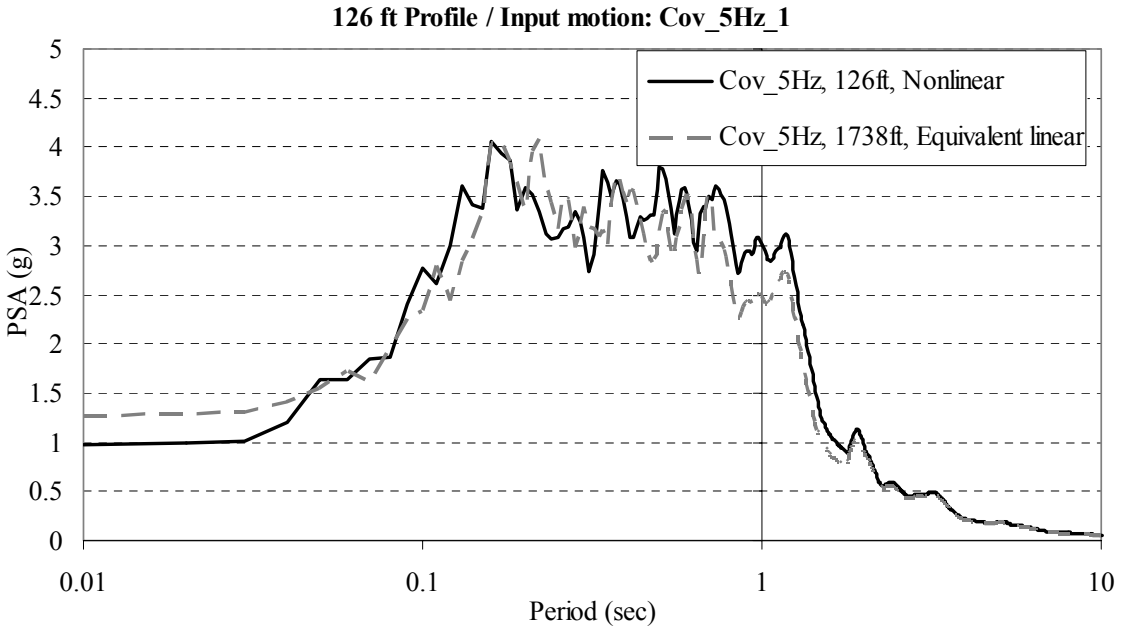

Figure 3-12. 126-ft profile using time histories generated using 5Hz case.

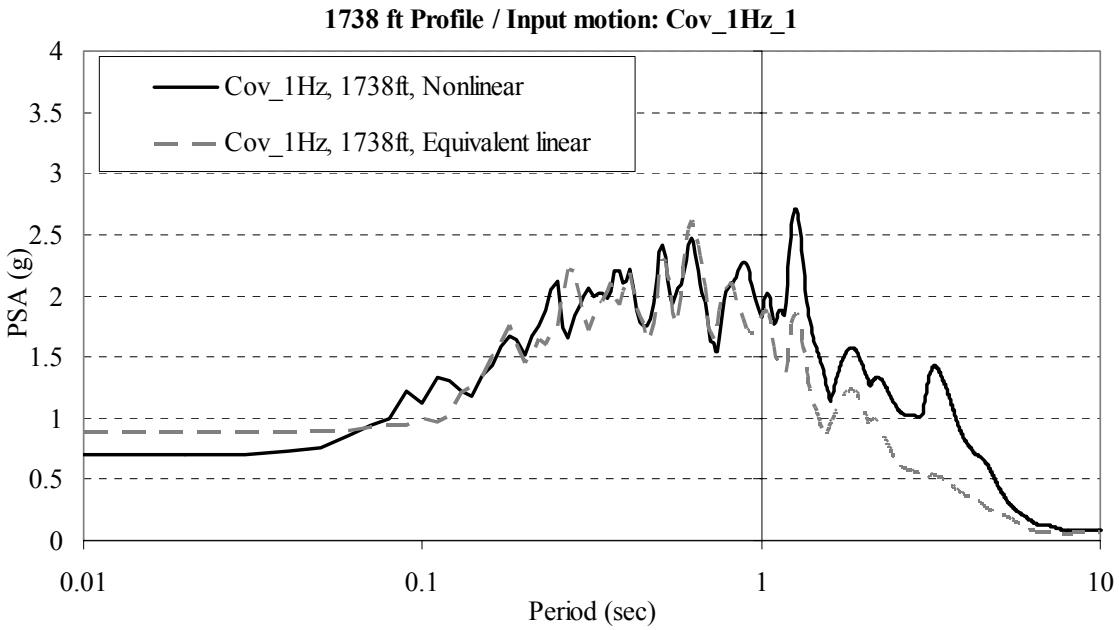

Figure 3-13. 1738-ft profile 126-ft profile using time histories generated using 1Hz case.

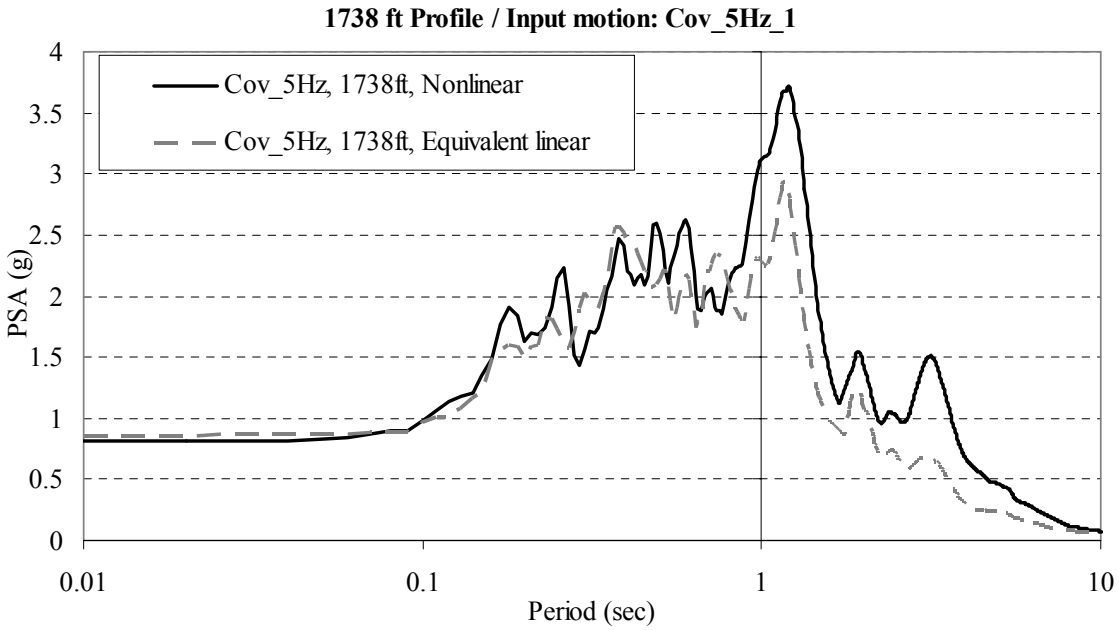

Figure 3-14. 1738-ft profile using time histories generated using 5Hz case.

4. Ground Motion Times Series and Probabilistic Seismic Hazard Analysis

4.1. Probabilistic seismic hazard analysis to simulate USGS hazard maps

The purpose of the proposed PSHA is to develop a suite of motions that as a sum results in the same hazard level as the USGS hazard maps. Identical methodology and assumptions as those used in development of the USGS hazard maps are used. The main framework developed by Wen and Wu (2001) is incorporated. Several important changes have been made to the procedure:

a) Implementation of the newest version of synthetic motion generation code SMSIM (Boore 2002), and

b) Representation of the NMSZ faults consistent with USGS hazard maps as three parallel fictitious faults.

Details of the proposed PSHA procedure are presented in the following and schematic flowchart is shown in Figure 4-1. The results of the simulations are compared to the 1996 USGS hazard maps for selected locations in the embayment.

4.2. Source characterization

USGS hazard maps define two types of sources, a) gridded seismicity and b) characteristic sources. The gridded seismicity sources are intended to cover the historical seismicity recorded. These sources represent seismicity from unknown faults to which a specific value of recurrence interval and magnitude size cannot be assigned. The characteristic sources represent sources at which the recurrence interval, magnitude, and geologic shape can be approximately estimated based on the geologic evidence. The gridded and characteristic sources are treated separately and added to the final seismic hazard. The details on how the two source types are simulated are described in the following sections.

4.2.1. Gridded seismic sources

The annual recurrence rate of earthquakes is based on seismicity database from USGS Open-File-Report 96-532 (Frankel et al. 1996). USGS seismicity data is defined for every 0.1° x 0.1° grid within central and eastern United States (Figure 4-2 and Figure 4-3). The database gives a, b, and m_{max}. A uniform value of 4.71 is used for m_{low} in the central and eastern United States. Using the four values, the bounded Gutenberg Richter recurrence relationship is defined (discussed in detail later). USGS uses the recurrence relationship to estimate the probabilities of various magnitudes to occur at the grid.

The proposed simulation procedure needs to generate actual sources that in sum agree with the recurrence relationship defined at each grid. The theory of probability is used to accomplish this goal. According to the probability theory, a sufficient number of random numbers generated will result in the mean value. The mean number in the

simulation is the seismicity (mean rate of the earthquakes to exceed m_{low}). The number of sources generated should be equal to the seismicity. The magnitude assigned to the generated sources should be consistent with the recurrence relationship of the grid.

The process of determining future sources is performed in the following two steps:

a. Number of earthquakes within each grid

For a Poisson process, the probability of a random variable N (number of occurrences of seismic events) occurring X times during a given time interval t (equivalent to PDF) is:

$$P\left[N = X\right] = \frac{\left(t\lambda_k\right)^X}{X!} e^{-t\lambda_k} \tag{4-1}$$

where λ_k is the annual occurrence rate of earthquakes with body wave magnitude higher than 5 and t is the period of simulation. Therefore, $t\lambda_k$ is the average number of occurrences of the event in the time interval. Then, the probability that the events occurring up to n_k times during t (equivalent to CDF, Figure 4-4) is:

$$P\left[N \le n_k\right] = \sum_{X=0}^{n_k} \frac{\left(t\lambda_k\right)^X}{X!} e^{-t\lambda_k} \tag{4-2}$$

The number of earthquakes within each grid can be determined by generating a random variable u_k, with a uniform distribution between 0 and 1, and relating it to the CDF as:

$$P\left[N \le n_{k-1}\right] < u_k \le P\left[N \le n_k\right] \tag{4-3}$$

which is equivalent to:

$$\sum_{X=0}^{n_k-1} \frac{\left(t\lambda_k\right)^X}{X!} e^{-t\lambda_k} < u_k \le \sum_{X=0}^{n_k} \frac{\left(t\lambda_k\right)^X}{X!} e^{-t\lambda_k} \tag{4-4}$$

Where X is the number of simulated events within the selected grid. The number of occurrences during the time interval is n_k. To result in the number of earthquakes within each grid that is identical to the mean seismicity, sufficient number of simulations is required. 9000 simulations of 10-year period are performed.

b. Magnitude characterization

The random number, generated to determine the number of earthquakes within each grid for the given period of simulation, is also used to determine the corresponding magnitudes using the following equation, which is derived from Gutenberg-Richter law with lower (m_{low}) and upper bound (m_{max}):

$$m_b = m_{low} - \log_{10}\left(1 - u_k\left(1 - 10^{m_{low} - M_{\max}}\right)\right) \tag{4-5}$$

c. Location selection

Within each grid, two random numbers of uniform distributions are chosen along latitude and longitude directions within each cell to randomize the location of the source.

4.2.2. Characteristic earthquakes

Characteristic earthquakes are assumed to occur in the NMSZ (Figure 4-5). USGS NMSZ fault geometries are used which consist of three fictitious faults, shown in Figure 4-6. The faults' contribution to the hazard are weighted such that the center fault has a 1/3 and each of the two outer faults has a 1/3 wt in 1996 maps (Figure 4-1). The characteristic events were not randomly generated as in simulating the gridded seismic sources. The recurrence rate of characteristic events is fixed at 1000 years in 1996 maps, the number of occurrences within the simulation period can be calculated. The period of simulation in this study is 90,000 years. The number occurrences of characteristic earthquakes are 90 for 1996 maps. Since the faults have different weights, the number of sources for each of the fault should be assigned accordingly. For 2002 maps, 30 sources should be generated at each fault.

For this study ground motions are simulated within a reference area (within 500 km from the site, except for characteristic earthquake) over a 10-year period using the tectonic and seismological data provided in Frankel et al. (1996). A total of 9000 simulation of 10-year period are carried out to provide sufficient number of ground motions for statistical analysis. The ground motions generated are then used to develop the uniform hazard response spectra.

USGS uses the closest distances to each of the three faults to calculate the cumulative seismic hazard at the site. This means that only a single scenario (single M and R) possible at each of the three fault. M = 8.0 is used for 1996 maps.

4.2.3. Ground motion time history development and estimation of ground motion parameter

The magnitude and location information from the source characterization process is used to generate synthetic ground motions using stochastic model SMSIM (Boore, 2000). In this study, the newest version of SMSIM (ver. 2.2) is incorporated (Boore, 2002).

For 2002 maps, point sources single corner and double corner models are used. Single corner and double corner models are assigned the same weight, both for gridded seismic sources and characteristic sources (Figure 4-1).

4.3. UHRS development

The procedure for developing the UHRS is shown in a flowchart in Figure 4-7. The response spectrum of each of the propagated ground motions are calculated and compiled. Each of the points in the response spectrum represents the ground motion parameter *Y*. The annual probability of the source exceeding a particular value y^* can be calculated using equation.

$$\lambda_k = \lambda_i \cdot P\left[Y > y^*\right] = \lambda_i \cdot \left[1 - F\left(\frac{y^* - Y}{\sigma_{\ln Y}}\right)\right] \tag{4-6}$$

where λ_i for all of the generated motions is 1/total simulation years; σ_{lnY} is the lognormal standard deviation, $\left[1 - F\left(\frac{y^* - Y}{\sigma_{\ln Y}}\right)\right]$ is CDF of Y to exceed y^*. The annual probability of occurrence is calculated for a range of y^*. This procedure is repeated for all of the ground motions generated. The results are summed up. From the summation of all probabilities,

the ground motion parameter corresponding to the desired design probability of exceedance is calculated.

4.4. Comparison with USGS hazard maps

The simulated UHRS at B/C boundary are compared to 1996 USGS mapped hazard and NEHRP Site B design response spectrum. USGS hazard maps provide 4 ground motion parameters (PGA, 0.2, 0.3, and 1.0 sec SA). The NEHRP Site B design spectrum is used to represent the hazard at other periods at B/C boundary. Seismic hazard corresponding to 2% and 10% in 50 years probability of exceedance seismic hazards are compared and provide a very good match.

The generated motions are representative of B/C boundary condition. To use them as input motion imposed at the bottom of the bedrock, the motions have to be converted back to the hard rock condition. The amplification of the motion at the B/C boundary is calculated using the transfer function shown in Figure 4-8. By applying the inverse of the transfer function, the motion at the hard rock can be calculated using the generated B/C boundary ground motions.

Step 1 Select number of 10-year period simulations (N)

Step 2 Source Characterization

Gridded seismicity sources

For each grid for 10-year-period:

a. Read seismicity information (a, b, M_{max} from *USGS seismicity database*) for selected grid. m_{low} is 4.71 everywhere in CEUS.

b. Randomly generate a uniformly distributed number u_k

c. Calculate number of occurrences within 10 years (n_k):

$$\sum_{X=0}^{n_k-1} \frac{(t\lambda_k)^X}{X!} e^{-t\lambda_k} < u_k \le \sum_{X=0}^{n_k} \frac{(t\lambda_k)^X}{X!} e^{-t\lambda_k}$$

where $t\lambda_k$ = mean seismicity (= 10 yr × $10^{(a-b\cdot m_{low})}$).

d. Determine magnitude for the generated sources

$$m_b = m_{low} - \log_{10}\left(1 - u_k\left(1 - 10^{m_{low} - M_{\max}}\right)\right)$$

Repeat steps ***a*** to ***d*** for all grids within reference area for N simulations.

Characteristic sources

a. Calculate the closest distance to the three NMSZ faults

b. Calculate number of occurrences for each NMSZ fault (N_{char}):

N_{char} = *(N× 10 yr) × 0.001/yr × 1/3 for each fault*

where 0.001/yr is the recurrence rate of characteristic earthquake; 1/3 is the weight of each NMSZ fault.

Step 3 Development of ground motion time history

Use the source information (M and R) to generate ground motion time history using *single-corner* frequency source model option in SMSIM (Boore, 2002)

Step 4 Develop UHRS

Figure 4-1. Flowchart for performing PSHA to simulate 1996 USGS hazard maps

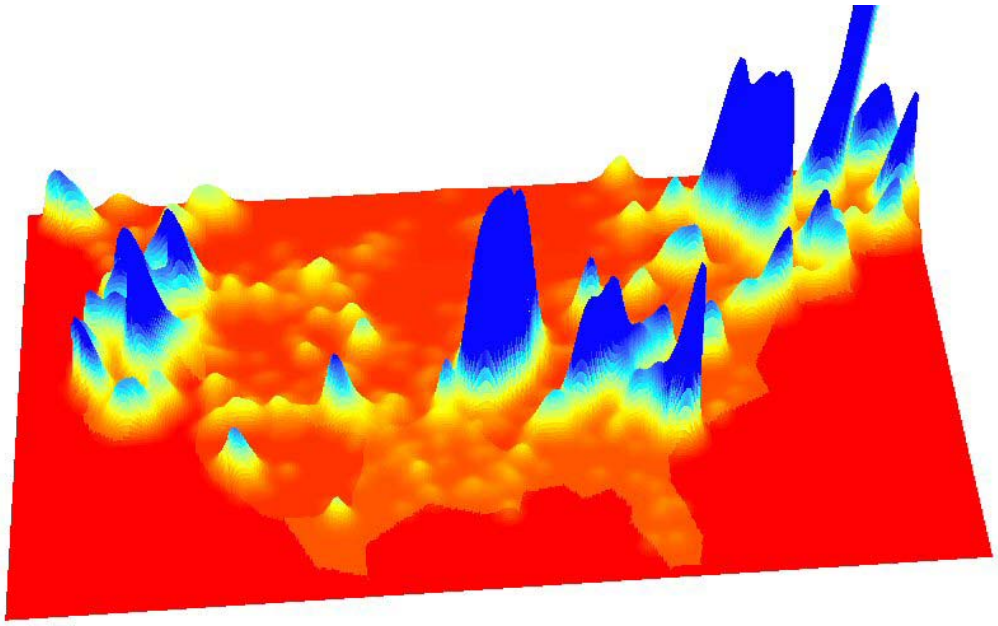

Figure 4-2. Seismicity of the United States.

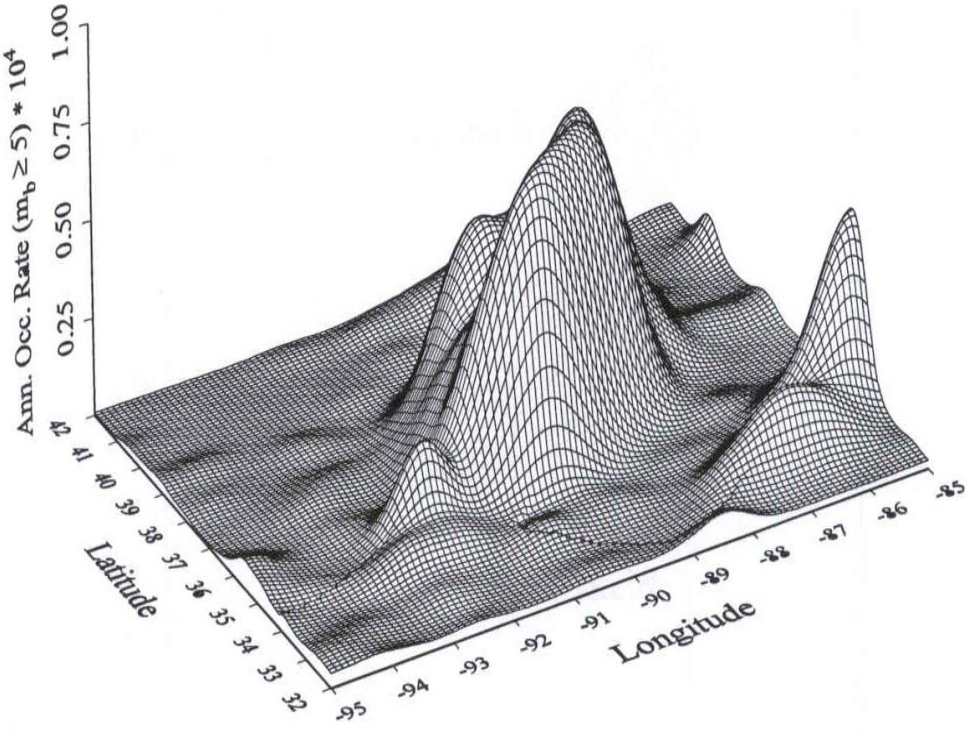

Figure 4-3. Seismicity in the Central and Eastern US.

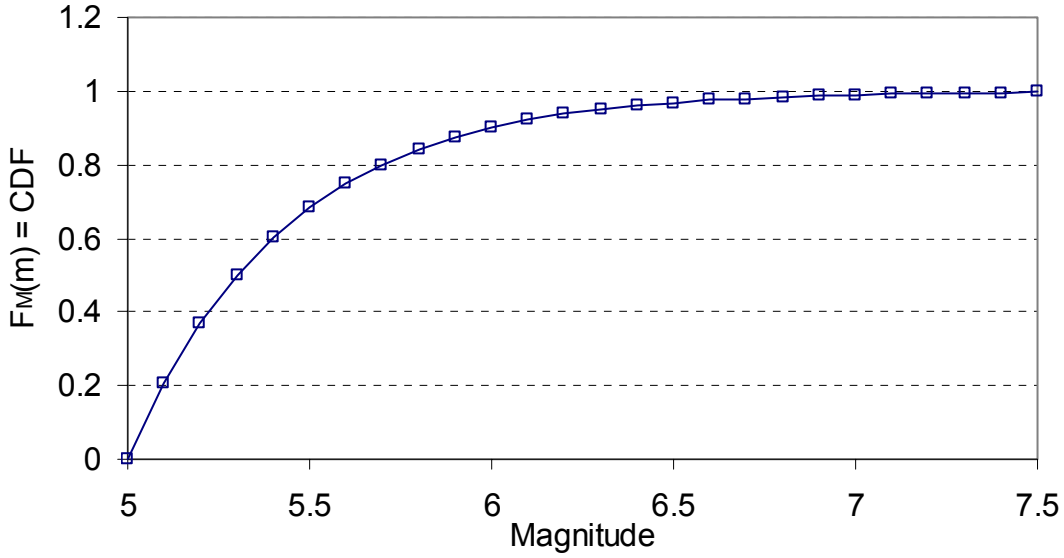

Figure 4-4. CDF of Bounded Gutenberg-Richter relationship (m_{low}=5, M_{max} =7.5).

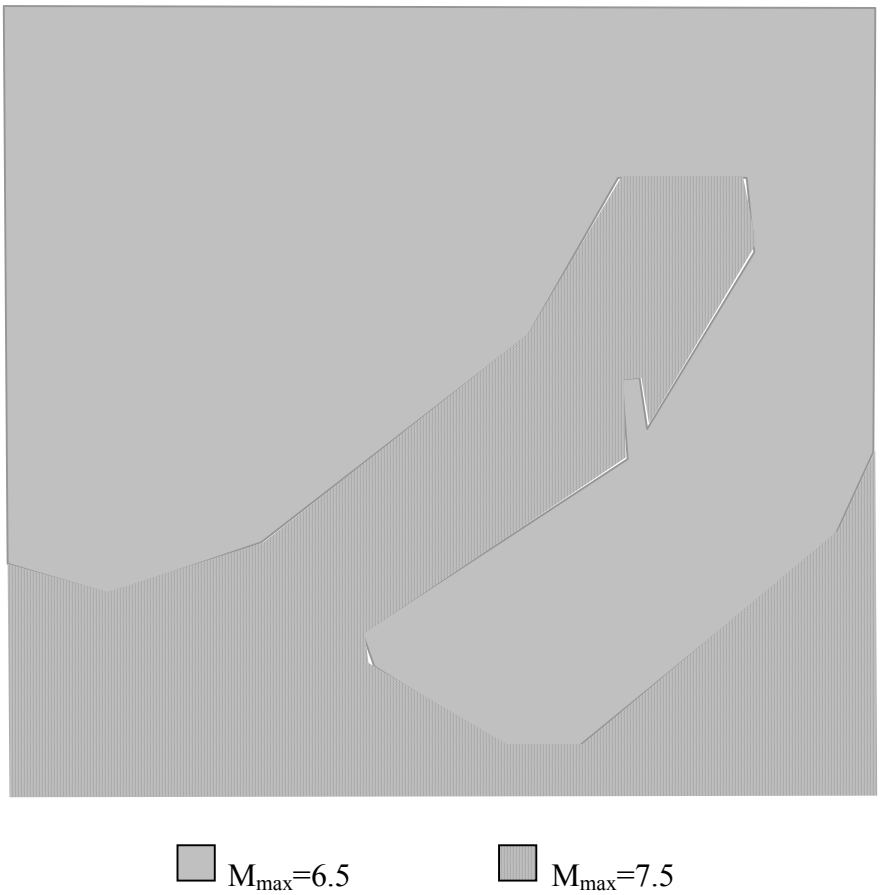

Figure 4-5. Contour map of M_{max} in the CEUS.

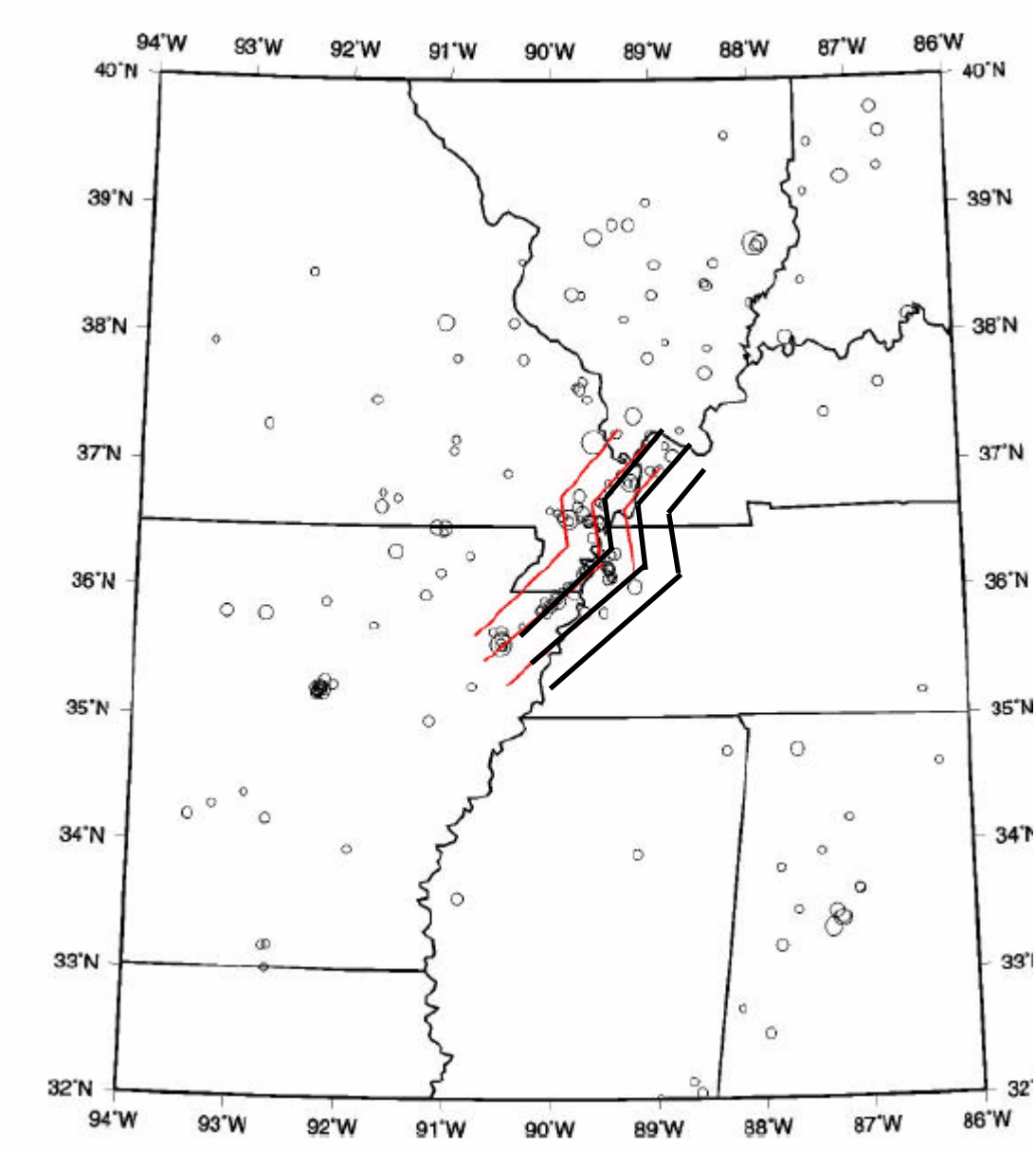

Figure 4-6. Three NMSZ fictitious faults used to define the characteristic earthquake in the Mississippi embayment

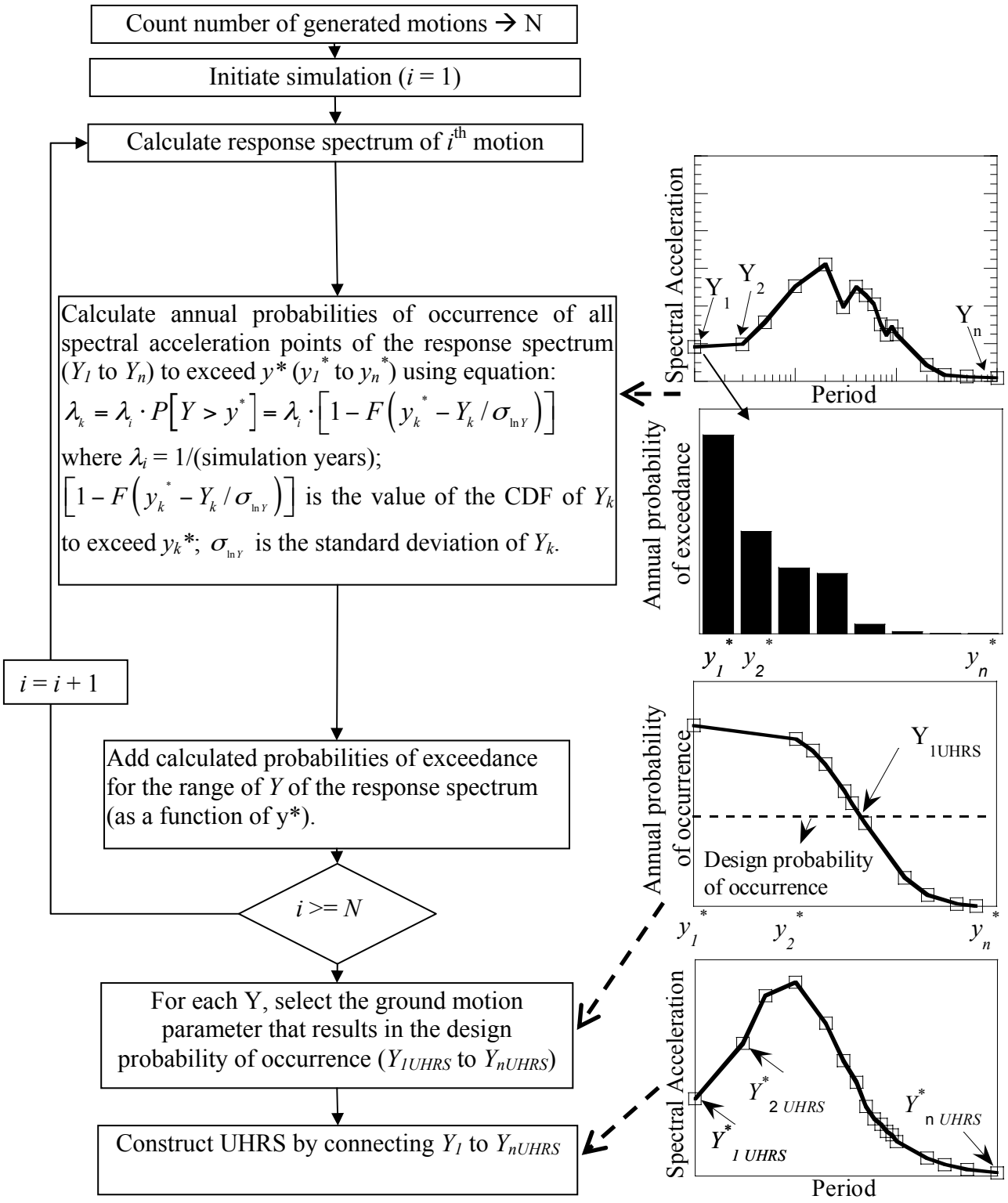

Figure 4-7. Flowchart for calculating UHRS.

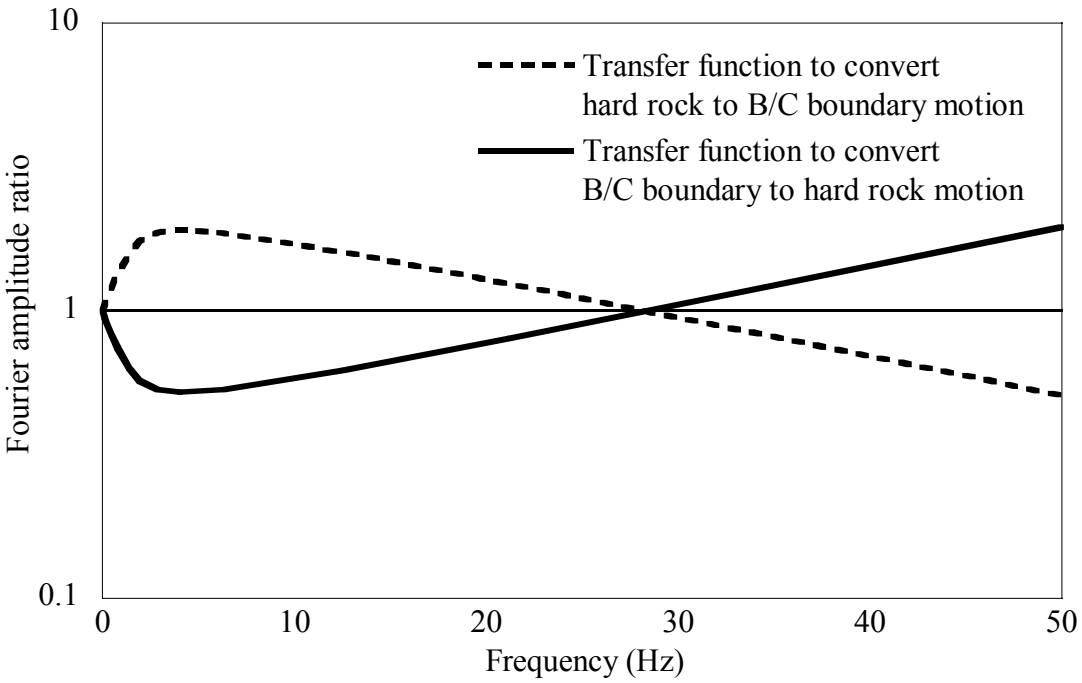

Figure 4-8. Transfer functions to convert hard rock to B/C motions and vise versa.

5. Estimated Site Factors

5.1. UHRS at Selected Sites

The results of PSHA with non-linear site effects using DEEPSOIL analyses are presented in Figure 5-1 through Figure 5-9 for 2% probability of exceedance in 50 years. Each graph inludes:

a) the USGS peak ground accelerations and spectral accelerations at 1.0 and 0.2 seconds at B/C boundary

b) NEHRP UHRS at B/C boundary

c) Simulated UHRS using the probabilistic seismic hazard analysis developed in Section 4 at B/C boundary

d) NEHRP UHRS corresponding to the site class for the studied site

e) Computed surface UHRS (after propagation through embayment deposit using DEEPSOIL) using generic soil profile. A proposed NEHRP style UHRS is also shown

f) Computed surface UHRS (after propagation through embayment deposit using DEEPSOIL) using site specific soil profile. A proposed NEHRP style UHRS is also shown

In general, for all sites except Paris, the computed/proposed UHRS are lower than those obtained using NEHRP recommended spectra. The computed HURS also show a shift towards longer period compared to NEHRP spectra.

5.2. Computed Site Factors

Site factors are computed using the proposed NEHRP style UHRS and shown in Table 5-1, Figure 5-10 and Figure 5-11. For comparison corresponding NEHRP factors, obtained from Table 2-3 and Table 2-4, are also shown.

From analysis of 10 sites, it is determined that NEHRP or NCHRP 12-49 site coefficients F_a are mostly conservative and maybe reduced for sites in West Tennessee. However, the values of F_v are reasonable and in some cases need to be increased slightly.

Pezeshk et al. (1998) considered the whole West Tennessee and determined the mean and the standard deviation for the amplification factors for peak ground acceleration, spectral acceleration at 1 second and 0.30 second. Table 5-2 provides the mean and the standard deviation of soil amplification factors obtained by Pezeshk et al.

(1998). It is of interest that amplification factors obtained in Pezeshk et al. (1998) were based on equivalent linear analysis and are close to the results of the current AASHTO Specifications for soil type II.

The results of this study are limited to the specific sites selected and the assumptions related to choices of material properties and input motions. They should not be generalized to other sites without conducting additional site-specific studies.

Table 5-1. Values of F_a and F_v for Study Sites.

Site Considered	N	Site Class	F_a NEHRP	F_a DEEPSOIL (generic Uplands profile)	F_a DEEPSOIL (site specific profile)	F_v NEHRP	F_v DEEPSOIL (generic Uplands profile)	F_v DEEPSOIL (site specific profile)
Covington	20	D	1.00	0.78	0.7	1.63	2.3	2.3
Jackson	33	D	1.10	0.75	0.65	2.45	2.4	2.8
Newbern	24	D	1.22	0.95	0.80	1.92	2.65	2.75
Paris	37	D	1.12	1.20	1.10	1.86	1.86	1.86
Route 14	20	D	1.00	0.72	0.62	1.60	2.47	2.80
Somerville	55	C	1.00	0.75	0.65	1.50	2.45	2.45
Trenton	20	D	1.00	0.78	0.68	1.60	2.35	2.35
Wynnburg	16	D	1.00	0.50	0.42	1.50	2.10	2.10
Brownsville	16	D	1.00	0.80	0.72	1.72	2.30	2.30

Table 5-2. Soil Amplification Factors from Pezeshk et al. (1998)

	PGA	0.3 Sec	1.0 Sec
Average Amplification Factors	1.036	0.922	1.329
Standard Deviation	0.617	0.688	0.714

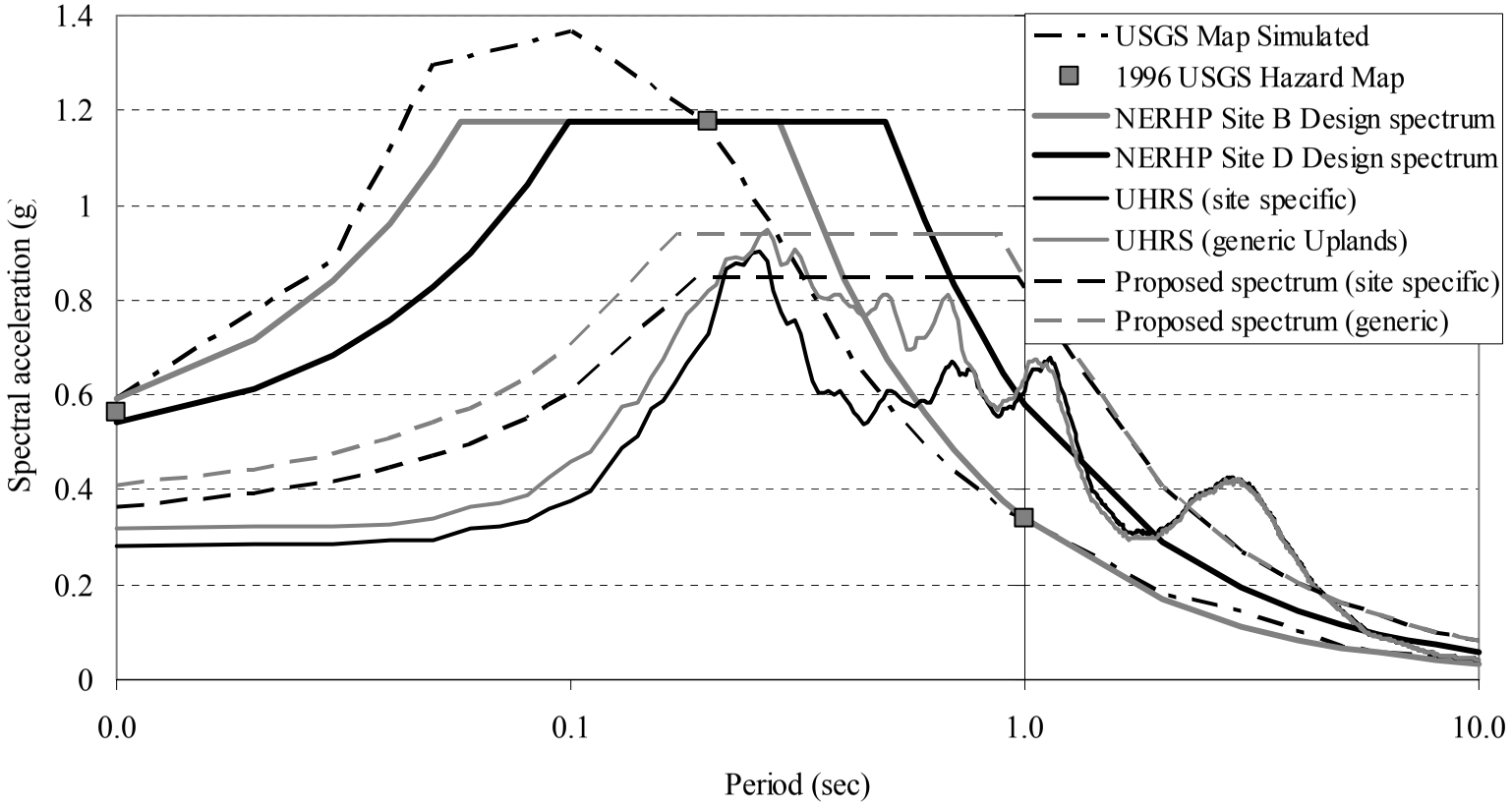

Figure 5-1. Response spectra for Brownsville.

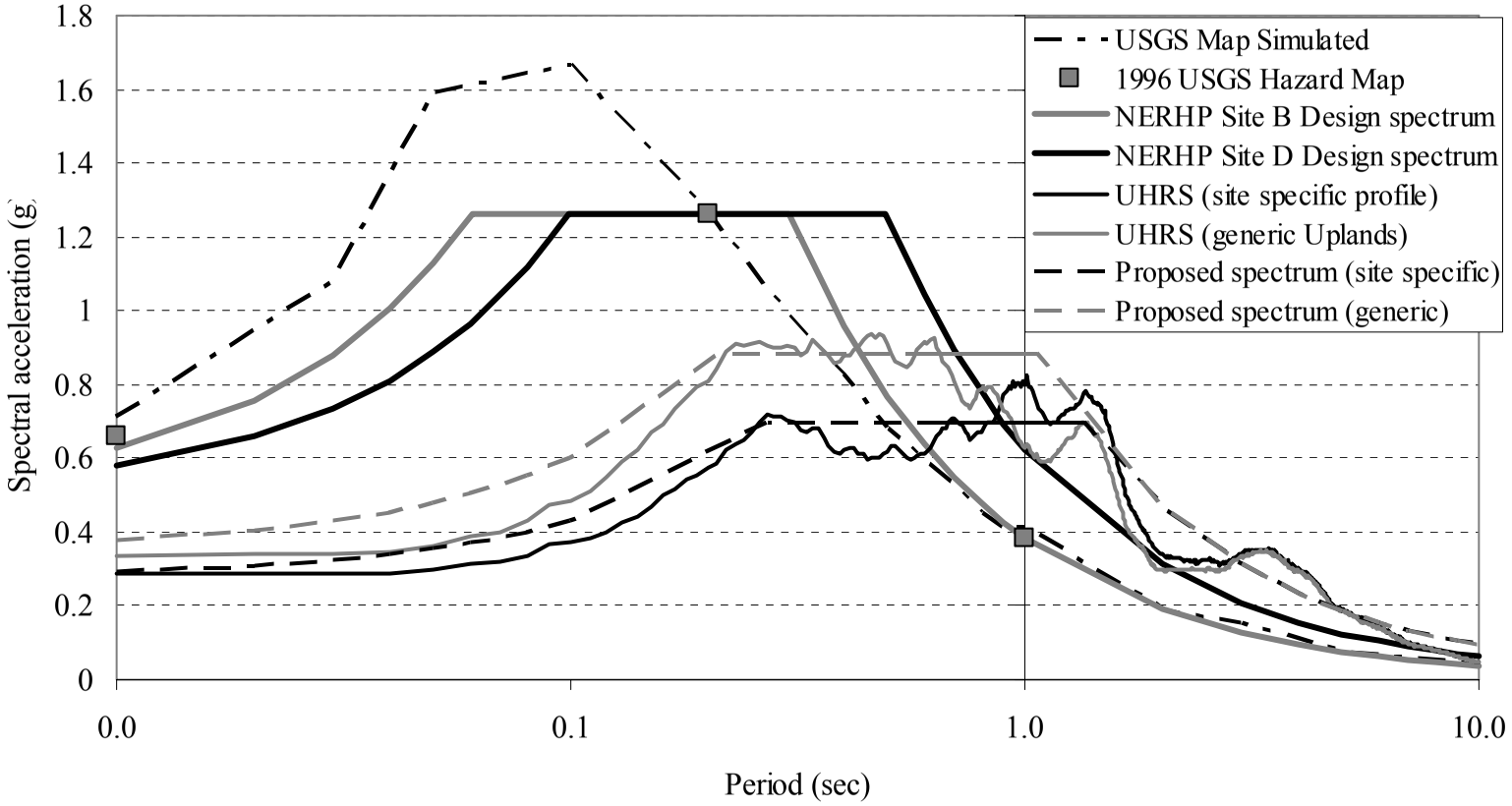

Figure 5-2. Response spectra for Covington.

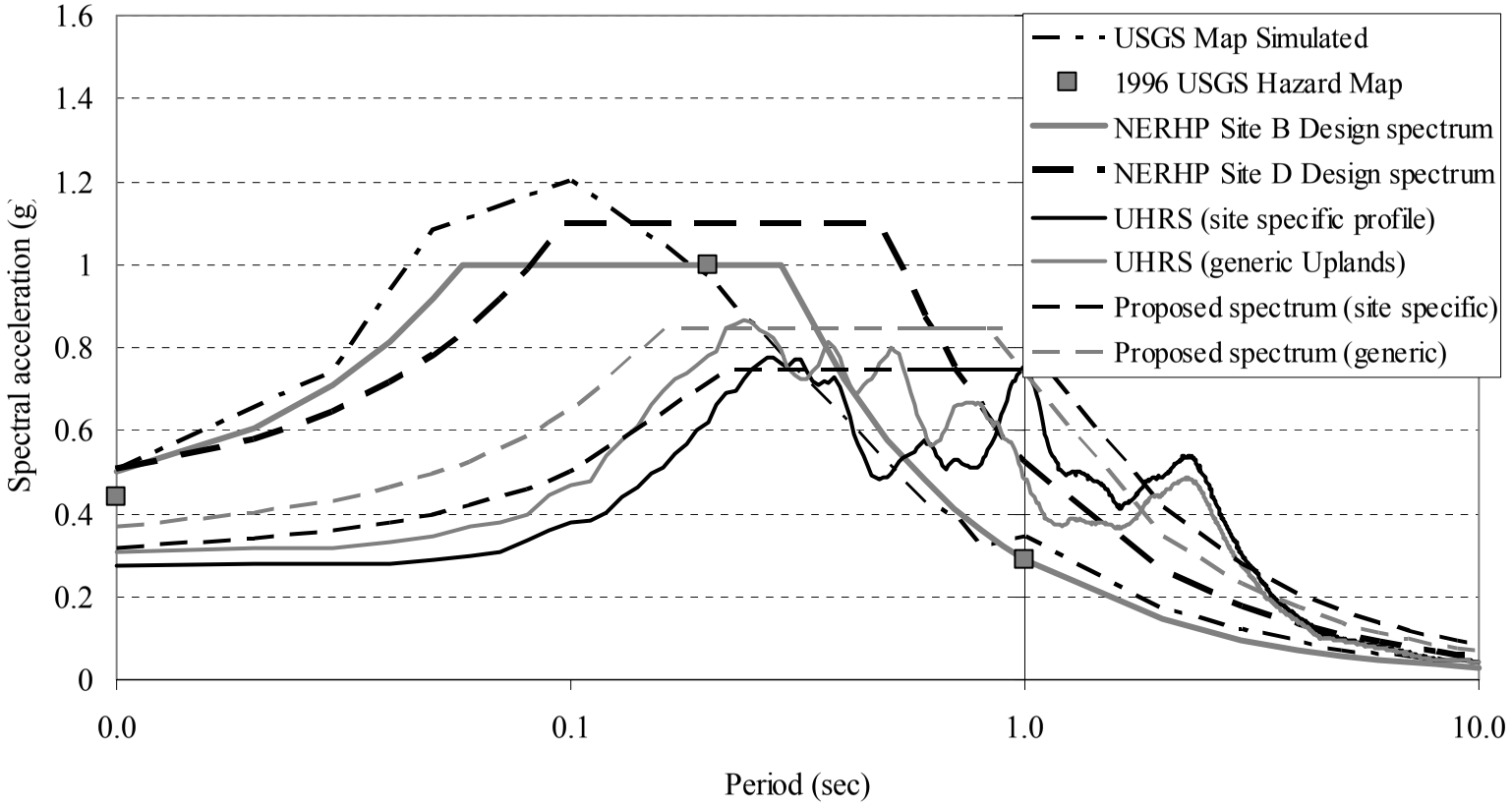

Figure 5-3. Response spectra for Jackson.

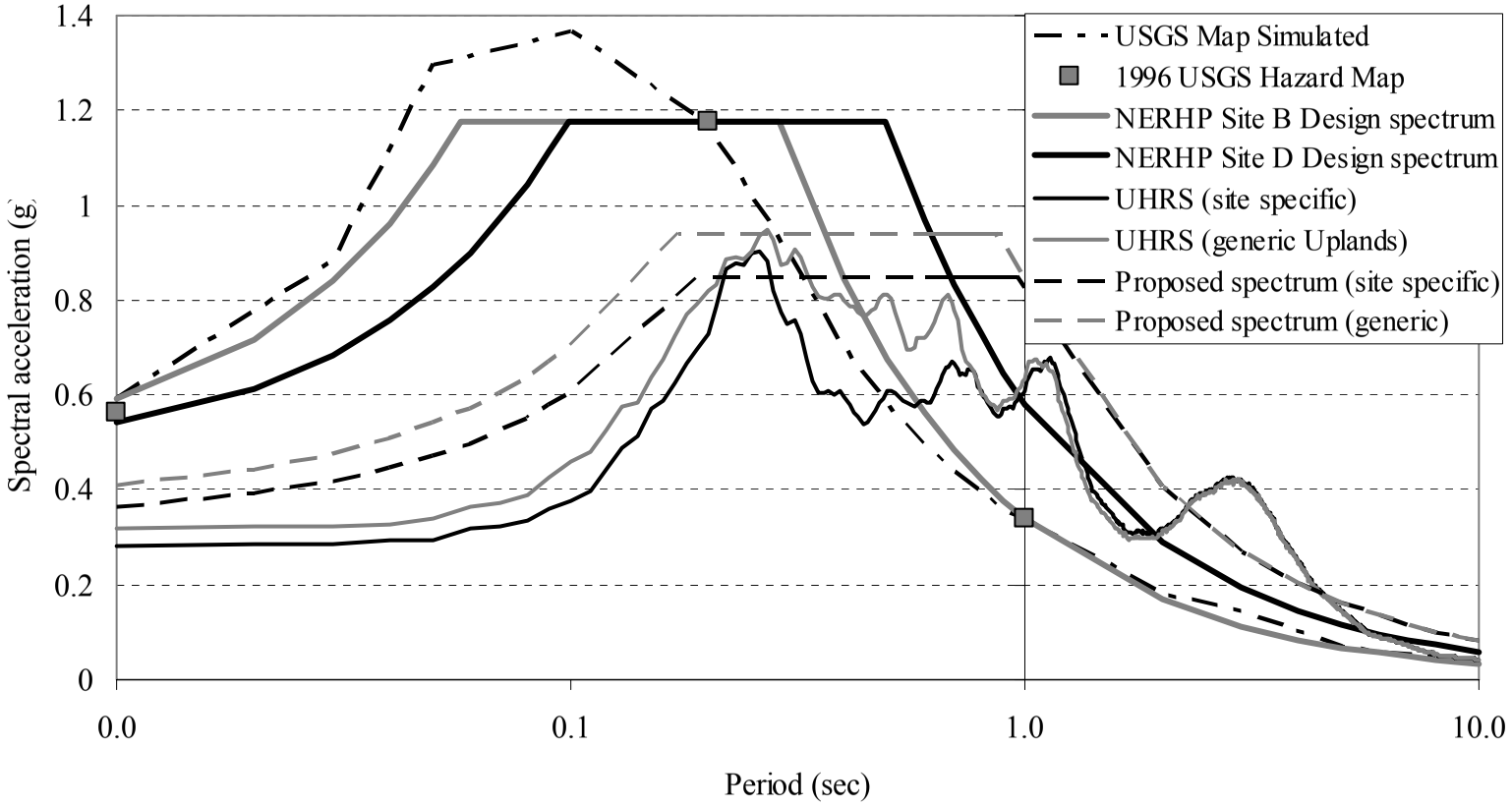

Figure 5-4. Response spectra for Newbern.

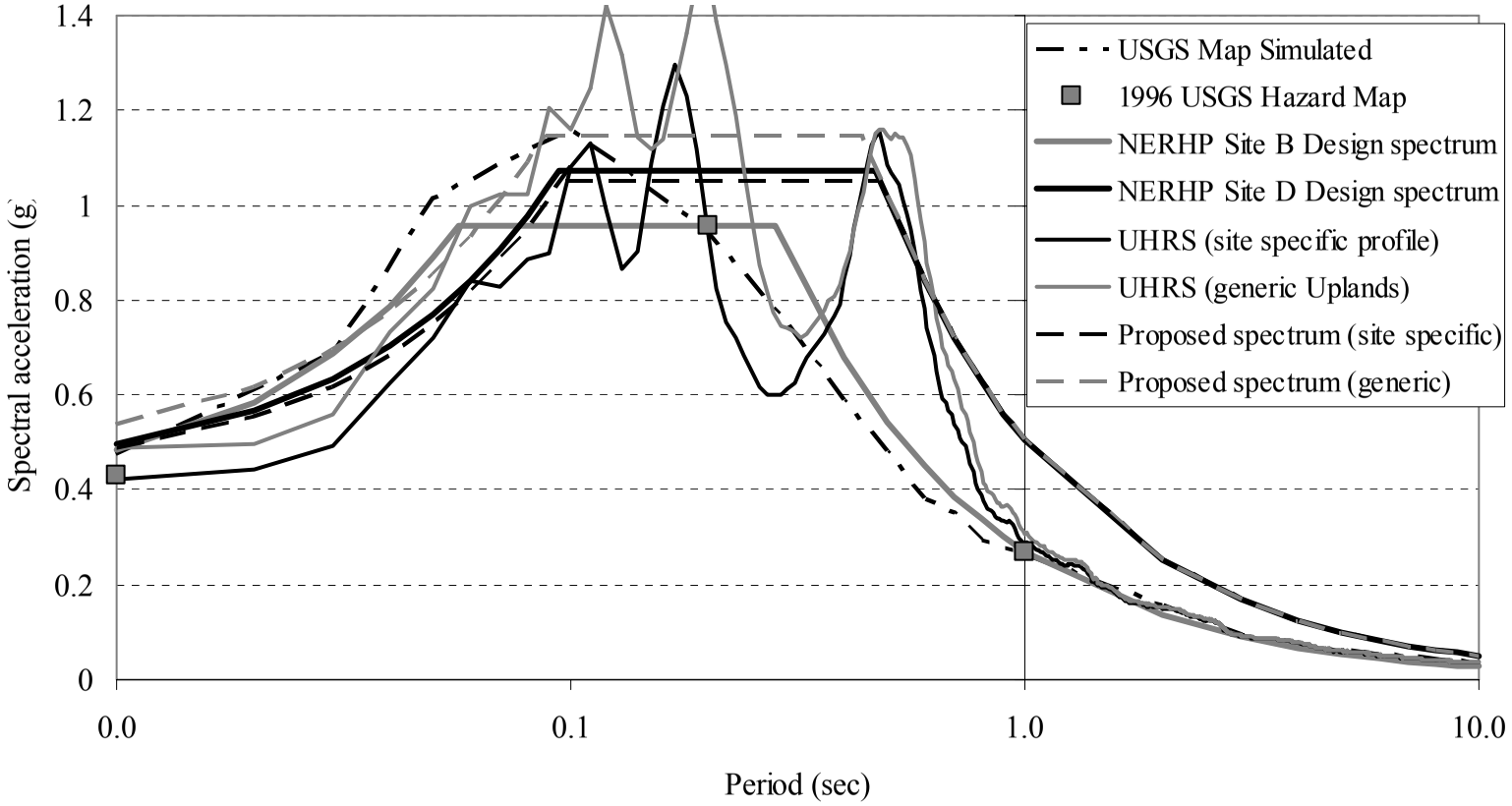

Figure 5-5. Response spectra for Paris.

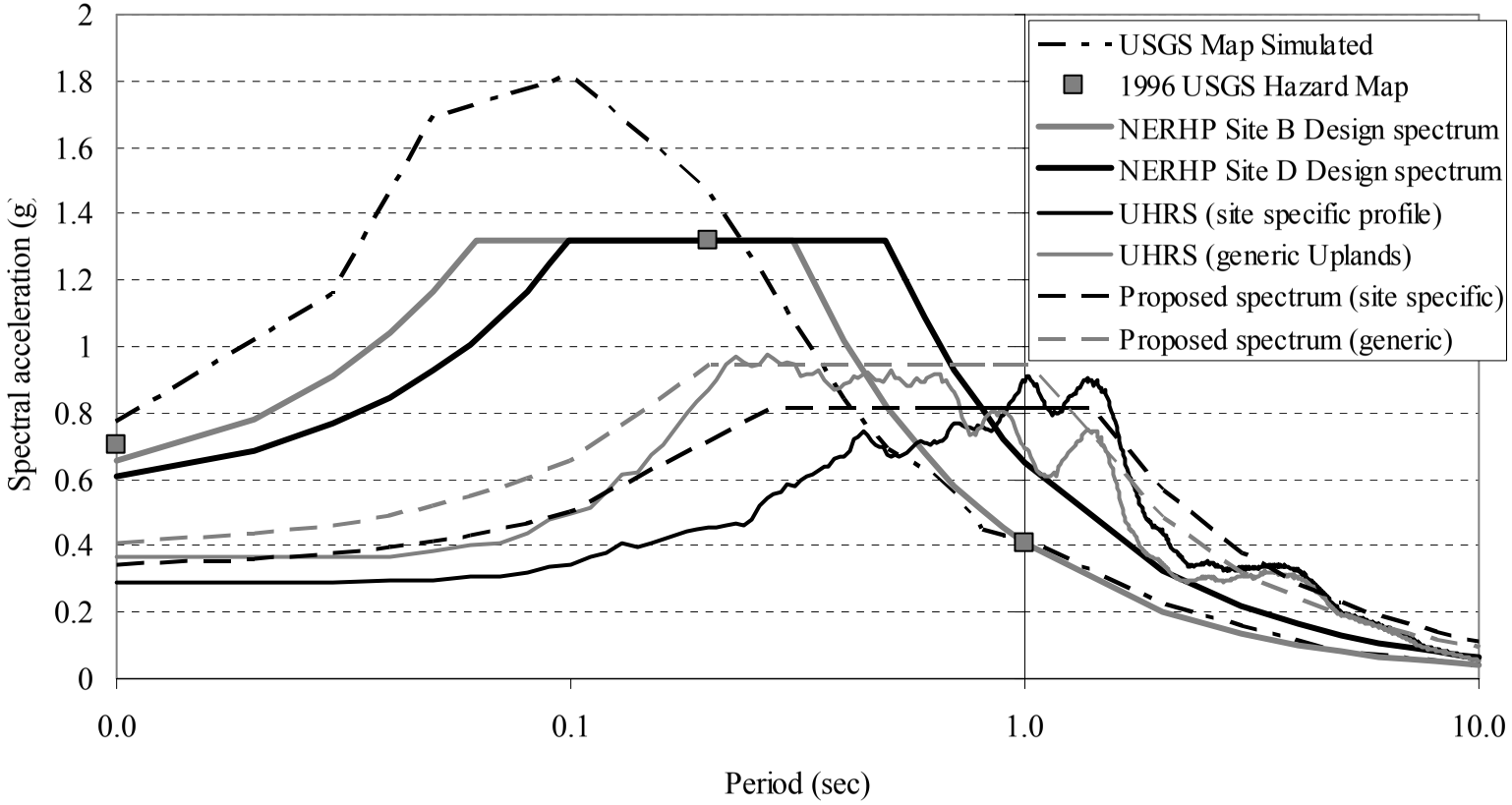

Figure 5-6. Response spectra for Route 14.

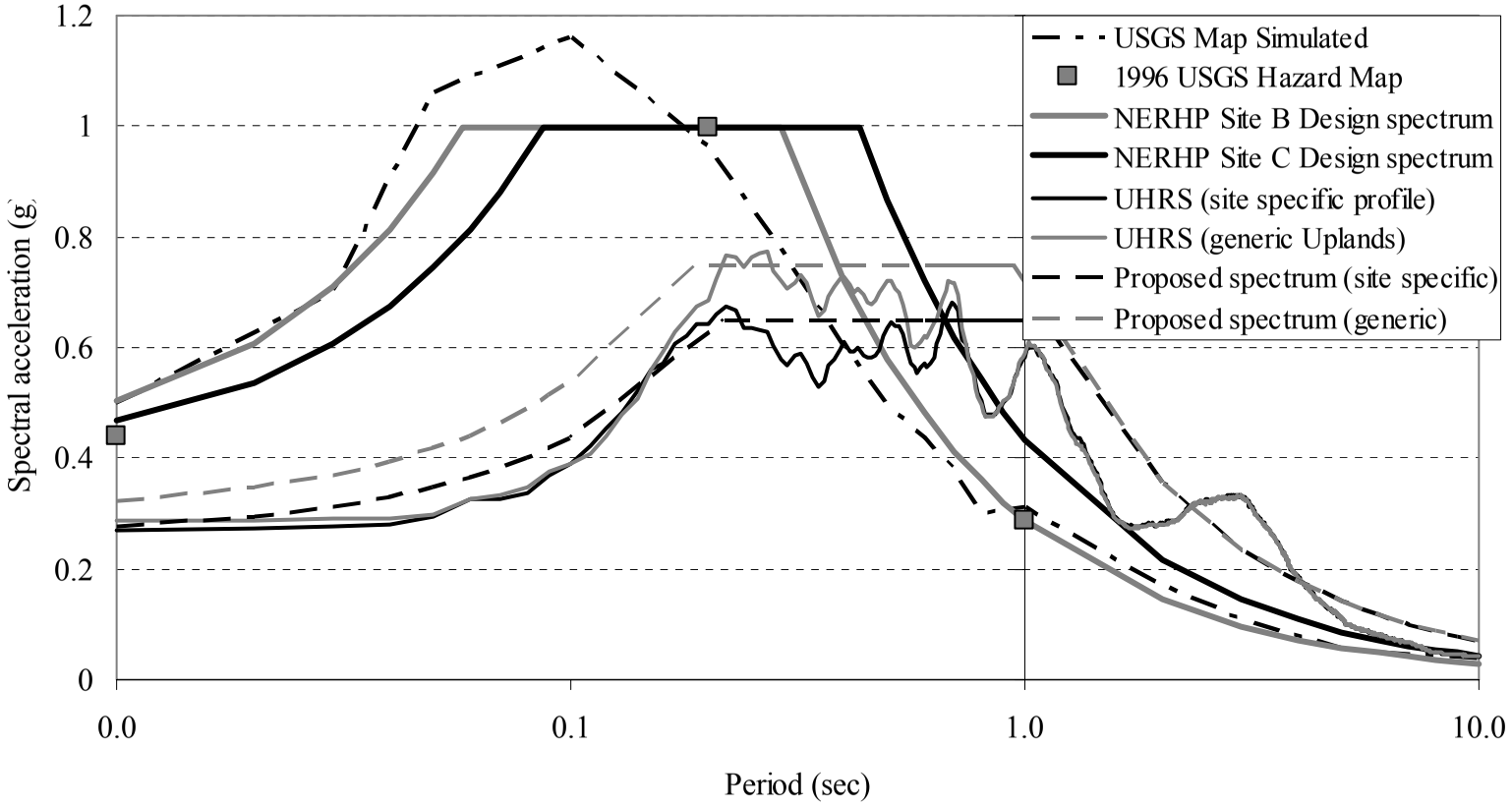

Figure 5-7. Response spectra for Somerville.

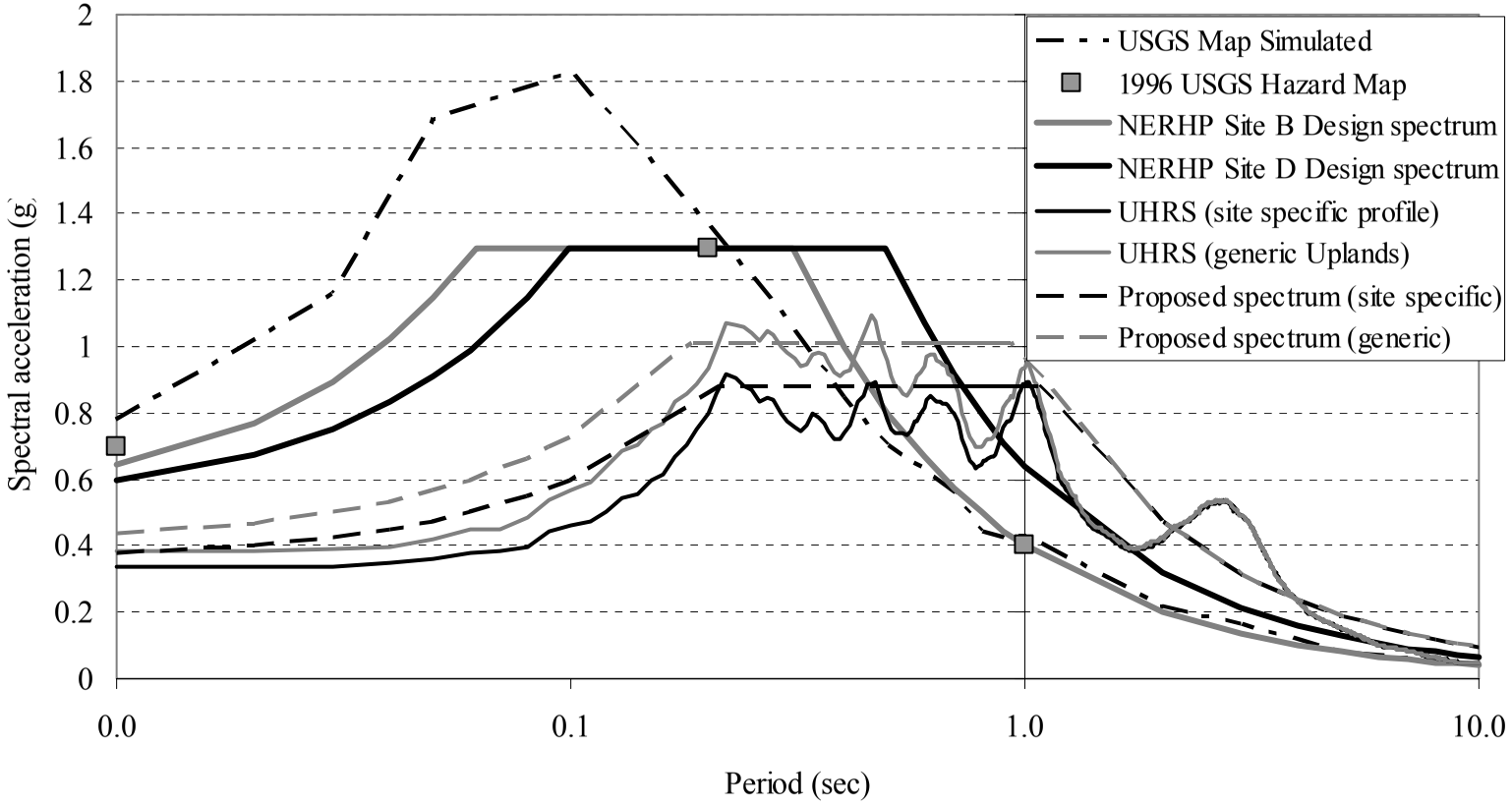

Figure 5-8. Response spectra for Trenton.

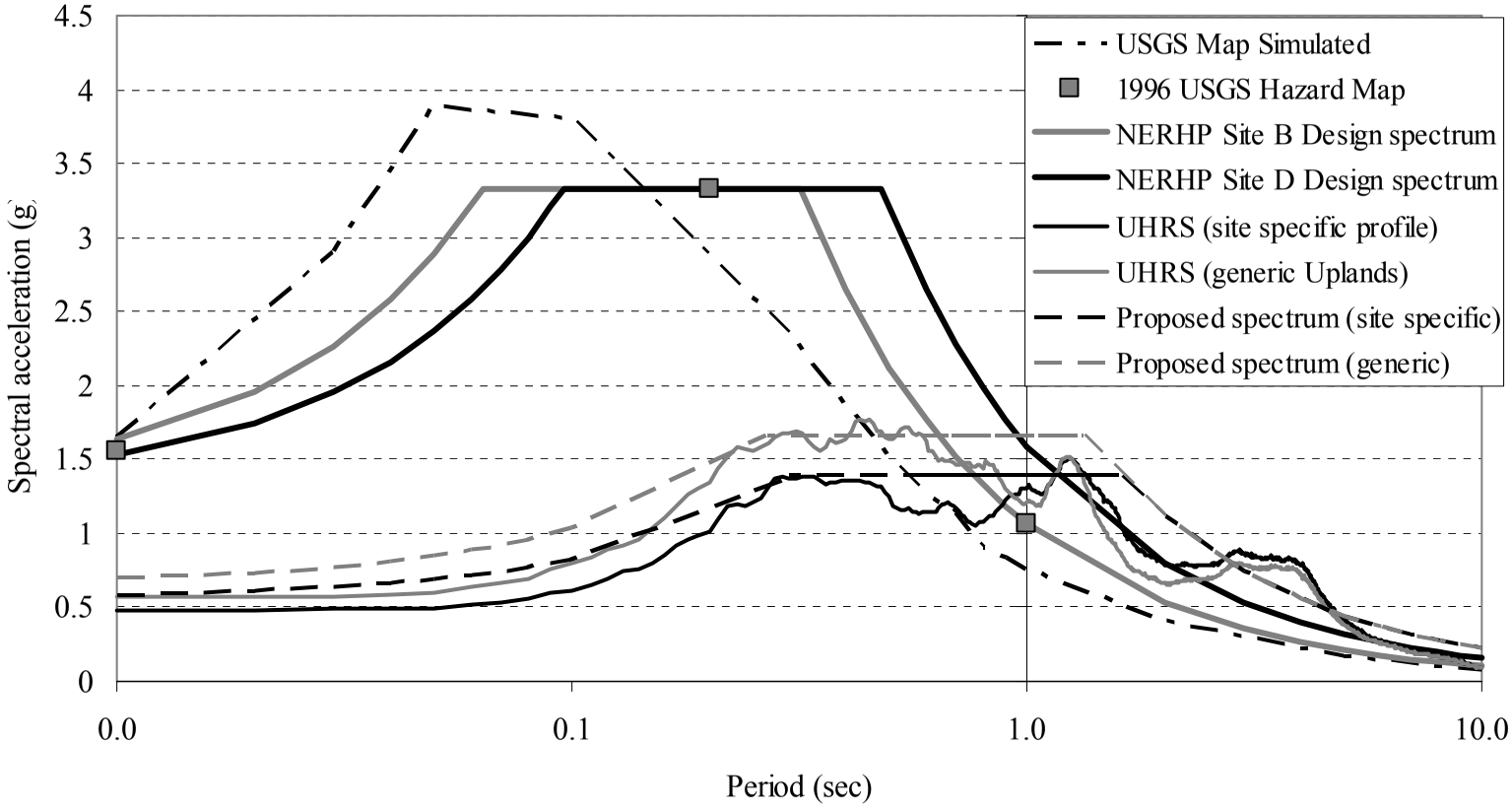

Figure 5-9. Response spectra for Wynnburg.

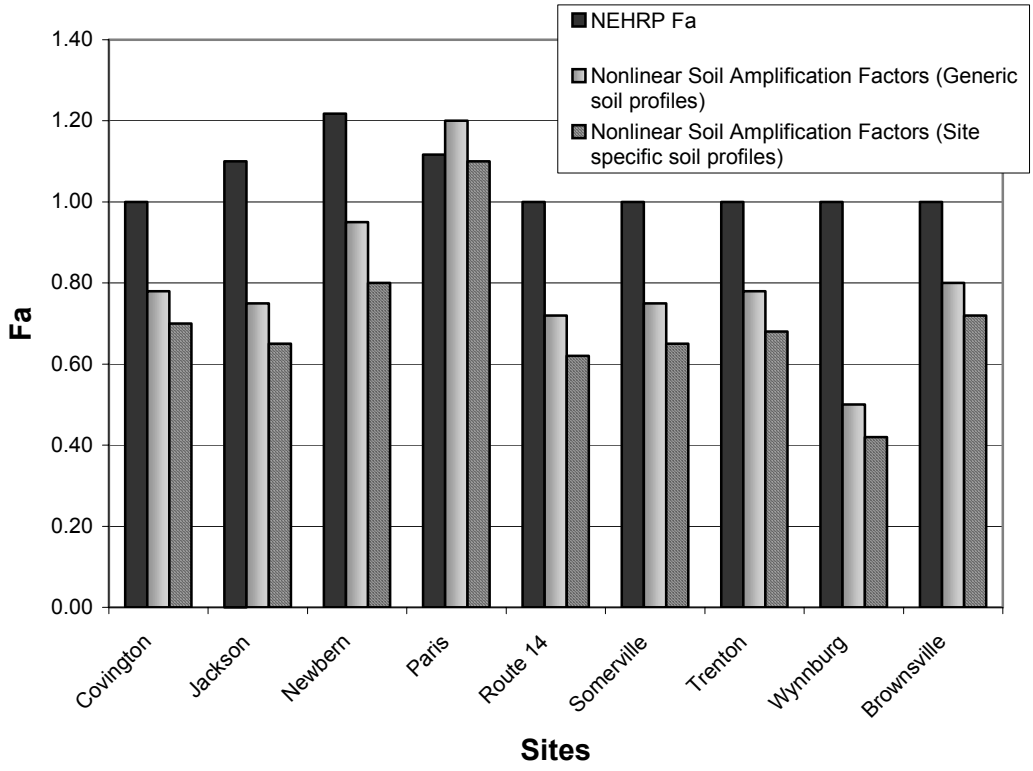

Figure 5-10. Values of F_a from DEEPSOIL results and NEHRP.

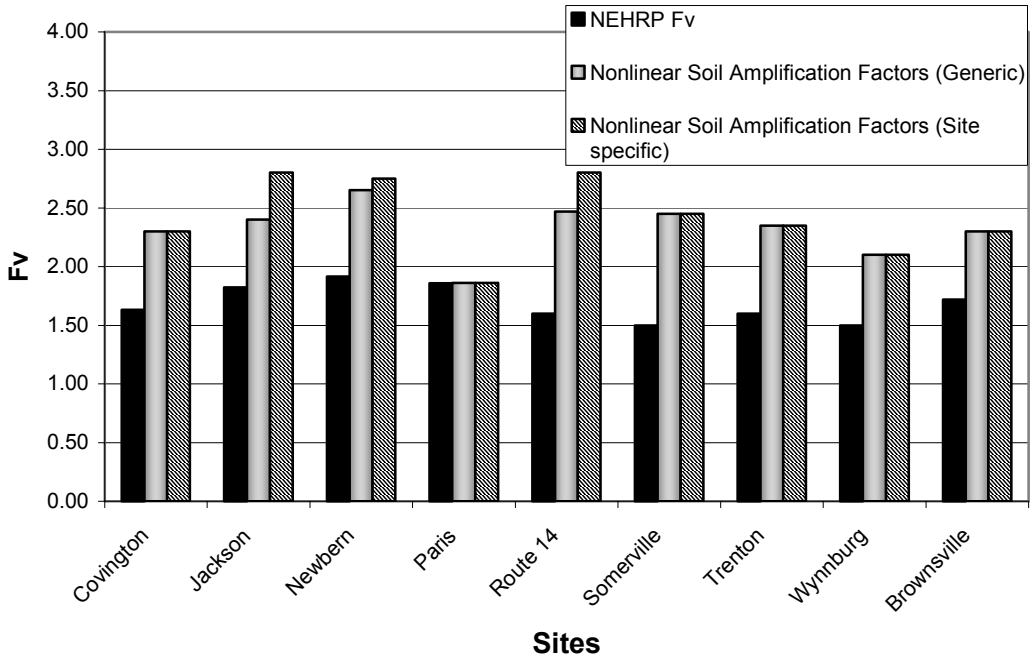

Figure 5-11. Values of F_v from DEEPSOIL results and NEHRP.

6. REFERENCES

Boore, D. M. (2000). "SMSIM Fortran programs for simulating ground motions from earthquakes: Version 1.87 Users' Manual." *96-80-A*, US Geological Survey.

Chang, T.S., Hwang, H., and Ng, K.W. (1989). "Subsurface conditions in Memphis and Shelby County, Tennessee." *NCEER-89-0021*, National Center for Earthquake Engineering Research, State University of New York at Buffalo, Buffalo, NY.

EPRI (1993). "Guidelines for determining design basis ground motions." *EPRI Tr-102293*, Electric Power Research Institute, Palo Alto, CA.

FEMA (1997). "NEHRP recommended provisions for seismic regulations for new buildings and other structures, Part I." 337p.

Frankel, A., Mueller, C., Perkins, D., Barnhard, T., Leyendecker, E., Safak, E., Hanson, S., Dickman, N., and Hopper, M. (1996). "National seismic hazard maps: Documentation June 1996." *OFR 960532*, US Geological Survey.

Hashash, Y.M.A. and Park, D. (2001). "Non-linear one-dimensional seismic ground motion propagation in the Mississippi embayment." *Engineering Geology*, 62(1-3), 185-206.

Hashash, Y.M.A. and Park, D. (2002). "Viscous damping formulation and high frequency motion propagation in nonlinear site response analysis." *Soil Dynamics and Earthquake Engineering*, 22(7), pp. 611-624.

Laird, J.P. and Stokoe, K. H. (1993). "Dynamic properties of remolded and undisturbed soil samples test at high confining pressure." *GR93-6*, Electric Power Research Institute.

Ng, K.W., Chang, T.S., and Hwang, H. (1989). "Subsurface Conditions of Memphis and Shelby County." *Technical Report NCEER-89-0021*, National Center for Earthquake Engineering Research, State University of New York at Buffalo, Buffalo, N.Y.

Park, D. and Hashash, Y.M.A. (2003). "Soil damping formulation in nonlinear time domain site response analysis." *Journal of Earthquake Engineering*, in press.

Pezeshk, S., Camp, C.V., Liu, L., J.M. Evans, J., and He., J. (1998). "Seismic Acceleration Coefficients For West Tennessee and Expanded Scope of Work for Seismic Acceleration Coefficients For West Tennessee Phase 2 - Field Investigation. Project Number TNSPR-RES116. Prepared for the Tennessee Department of Transportation and the U.S. Department of Transportation Federal Highway Administration." *Project Number TNSPR-RES116*, University of Memphis.

Romero, S., Hebeler, G., and Rix, G.J. (2001)."Recommended reference profile for Memphis, Tennessee." Engineering Geology,http://mae.ce.uiuc.edu/Research/GT-1/RRP.htm

Romero, S.M. and Rix, G.J. (2001). "Ground motion amplification in the Upper Mississippi Embayment." *GIT-CEE/GEO-01-1*, National Science Foundation Mid America Center, Atlanta.

Van Arsdale, R.B. and TenBrink, R.K. (2000). "Late Cretaceous and Cenezoic Geology of the New Madrid Seismic Zone." *Bulletin of the seismological society of America*, 90(2), 345-356.

Wen, Y. K. and Wu, C.L. (2001). "Uniform hazard ground motions for Mid-America Cities." *Earthquake spectra*, 17(2), 359-384.